

N 62 10013

NASA TN D-1178

NASA TN D-1178



TECHNICAL NOTE

D-1178

ANALYSIS OF THE "RANGE AND RANGE RATE" TRACKING SYSTEM

F. O. Vonbun

Goddard Space Flight Center
Greenbelt, Maryland



NATIONAL AERONAUTICS AND SPACE ADMINISTRATION
WASHINGTON

February 1962



ANALYSIS OF THE "RANGE AND RANGE RATE" TRACKING SYSTEM

by
F. O. Vonbun
Goddard Space Flight Center

SUMMARY

The "Range and Range Rate" ($r_j + \dot{r}_j$) System in its very simplest form is described. In particular, the errors in position and velocity are treated using pessimistic values of the measured quantities r_j and \dot{r}_j . Thus, a realistic evaluation of tracking qualities can be made for different orbits over certain tracking stations. The Range and Range Rate System briefly described in this report is a high precision tracking system.

Knowledge of the uncertainty in position δ_{x_i} is important, but knowledge of the uncertainty of the velocity vector $\delta_{\dot{x}_i}$ is of the utmost importance. Thus the use of coherent Doppler measurements to determine the velocity has a great advantage over any pulsed system and, in addition, permits extremely narrow frequency bands (in the order of 10 to 100 cps) to be employed, reducing the power requirements considerably.

The basis for using range r_j and range rate \dot{r}_j only is the fact that r_j and \dot{r}_j can be measured to very high precision, thus furnishing \vec{r} and $\dot{\vec{r}}$ with low errors. The nature of these errors is discussed.

BLANK PAGE

CONTENTS

	Page
Summary	i
INTRODUCTION	1
PRINCIPLE OF THE RANGE AND RANGE RATE SYSTEM	2
GENERAL THEORY OF THE SYSTEM	5
TRACKING ERRORS	8
Errors in Position	8
Errors in Velocity	17
Influence of the Troposphere and Ionosphere	27
CONCLUSIONS	27
ACKNOWLEDGMENTS	28
References	29
Appendix A - Details of the Satellite Position Errors	31
Appendix B - Details of the Satellite Velocity Errors	45

ANALYSIS OF THE "RANGE AND RANGE RATE" TRACKING SYSTEM

by
F. O. Vonbun
Goddard Space Flight Center

INTRODUCTION

The primary objective of a tracking system is to determine the position vector $\vec{r}(t)$ and velocity vector $\vec{v} = \dot{\vec{r}}(t)$ of an object moving in space. The "Range and Range Rate" ($r_j + \dot{r}_j$) System briefly described in this report is a high precision tracking system. The necessity for such a system, capable of determining a point in space \vec{r} and its velocity $\vec{v} = \dot{\vec{r}}$ within very small limits, originates from the increasingly sophisticated requirements for missile and satellite tracking. This is particularly true in the testing of precise guidance systems for rockets and space vehicles.

The position vector \vec{r} can be determined in three ways:

- (1) with a radar, which measures the range $|\vec{r}| = r$, the azimuth angle α , and the elevation angle ϵ ;
- (2) with a system (such as an interferometer) which measures angles and range separately;
- (3) with a system which measures ranges $|\vec{r}_j| = r_j$ only. Here, of course, at least 3 ground stations ($j = 3$) are necessary to determine a point in space (Figure 1). This system is known as the Range and Range Rate Tracking System.

When the vector $\vec{r} = (x_i)$, $i = 1, 2, 3$, has been determined, the time derivative $\dot{\vec{r}} = \vec{v} = (\dot{x}_i)$ immediately gives the velocity of the object. This information is obtained directly from Doppler measurements.

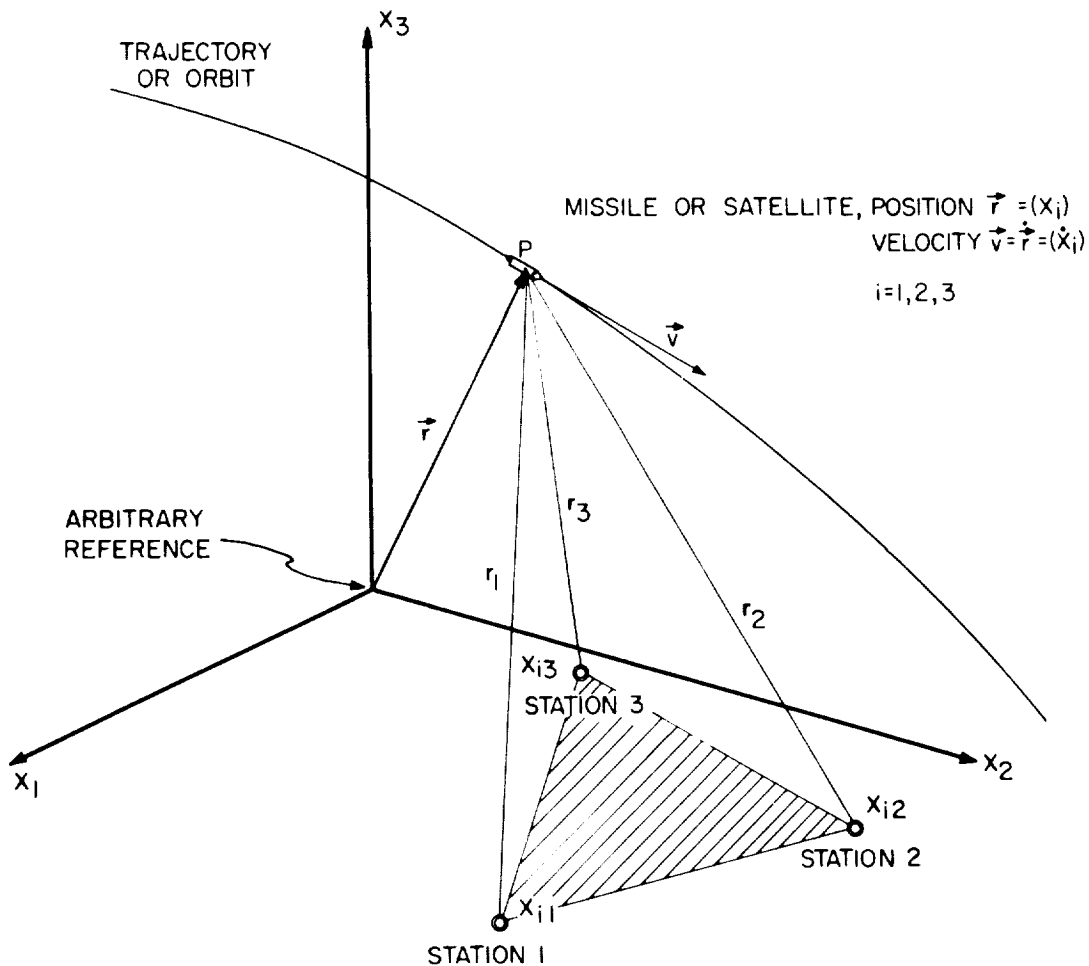


Figure 1 - General satellite and station geometry

PRINCIPLE OF THE RANGE AND RANGE RATE SYSTEM

The simplest way to determine the position and velocity vectors of a point in space is to measure six scalar quantities: range r_j and range rate \dot{r}_j ($j = 1, 2, 3$) from three locations (Figures 1 and 2). In general, the most precise and, at the same time, the most simple measurements that can be made are measurements of time and frequency. From such measurements, r_j and \dot{r}_j can be derived as follows.

The range can be determined simply by measuring the travel time of an electromagnetic wave. Knowledge of the wave propagation velocity (References 1 and 2) of this wave then gives the distance. This can be done by means of a pulse, as with radar, or by measuring the phase of a wave traveling from a transmitter to the spacecraft and back.

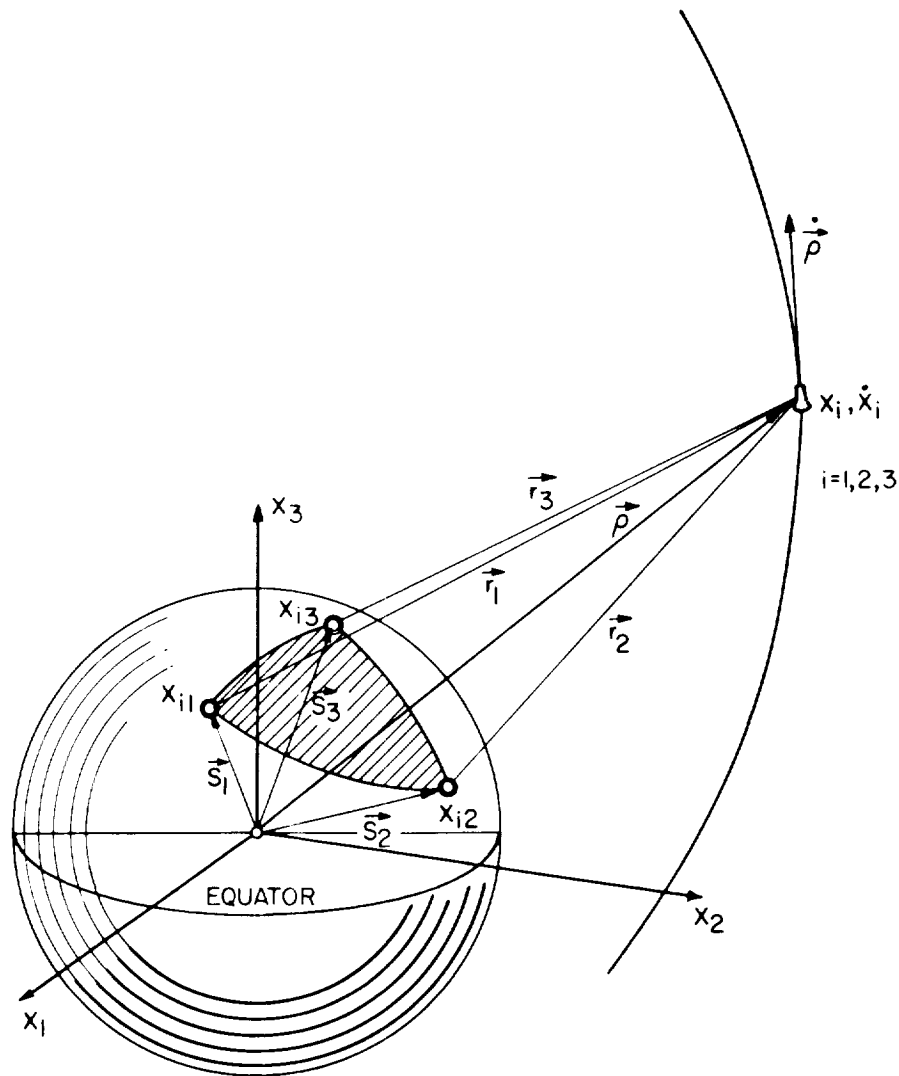


Figure 2 - Earth-centered coordinate system and station geometry

The latter principle, called sidetone ranging, is applied here. To resolve ambiguities connected with any phase measurement, a carrier with a frequency ν_0 is modulated with different frequencies, say $\nu_1, 5\nu_1, 5(5\nu_1)$, and so on. Measuring the phases of these related frequencies permits the determination of the r_j 's. This is, in principle, a time measurement.

Since the carrier ν_0 is a CW signal, its Doppler shift $\Delta\nu_{0j}$ (at the j^{th} station) can be measured very accurately, particularly when frequencies of $\nu_0 \geq 1\text{Gc}$ are being used. (The effects of the ionosphere are then small.) Since the Doppler shift is proportional to the range rate \dot{r}_j , the range rate can also be measured with great precision, provided that the short-time stability of the oscillator during the travel time (≈ 3 seconds to the

moon, 300 seconds to Venus, and 600 seconds to Mars) of the wave is very good, say in the order of one part in 10^9 to 5 parts in 10^{10} . It is therefore quite natural to use these quantities (r_j and \dot{r}_j) for tracking.

The position vector \vec{r} (Figure 1) can be written

$$\vec{r} = r \cdot \vec{r}^0$$

or

$$\vec{r} = \begin{bmatrix} x_1 \\ x_2 \\ x_3 \end{bmatrix} = (x_i), \quad i = 1, 2, 3 \quad (1)$$

where

$r = |\vec{r}|$ is the magnitude

$\vec{r}^0 = \vec{r}/r$ is the unit position vector.

A radar measures r and \vec{r}^0 . The unit vector \vec{r}^0 is determined from two angular measurements, namely azimuth α and elevation ϵ . Because the errors* $\delta\alpha$ and $\delta\epsilon$ associated with α and ϵ are fairly large (Reference 3), the total error in the position vector \vec{r} determining the point P in space is large. The resulting error ellipsoid is highly eccentric.

As an example, consider an FPS-16 radar (Reference 3) with $\delta r = \pm 10$ m and $\delta\alpha = \delta\epsilon \pm 0.2$ mrad. For a distance of 1000 km the error components perpendicular to \vec{r} are approximately $2 \times 10^{-4} \times 10^6 = 2 \times 10^2$ m, giving the eccentric ellipsoid shown approximately in Figure 3. The velocity error for distances of 1000 km and higher will amount to tens of m/sec because of the fairly large angular errors $\delta\epsilon$ and $\delta\alpha$. At a distance of 8000 km, typical errors for a large (such as 50 seconds) smoothing time would be 10 to 30 m/sec (Reference 4).

In view of these angular errors and their influence in fixing P, the complete elimination of any angular measurement will improve the situation considerably. The Range and Range Rate System accomplishes this.

*The notation δ refers to uncertainty in the measurements, whereas η refers to the rms errors obtained from least squares.

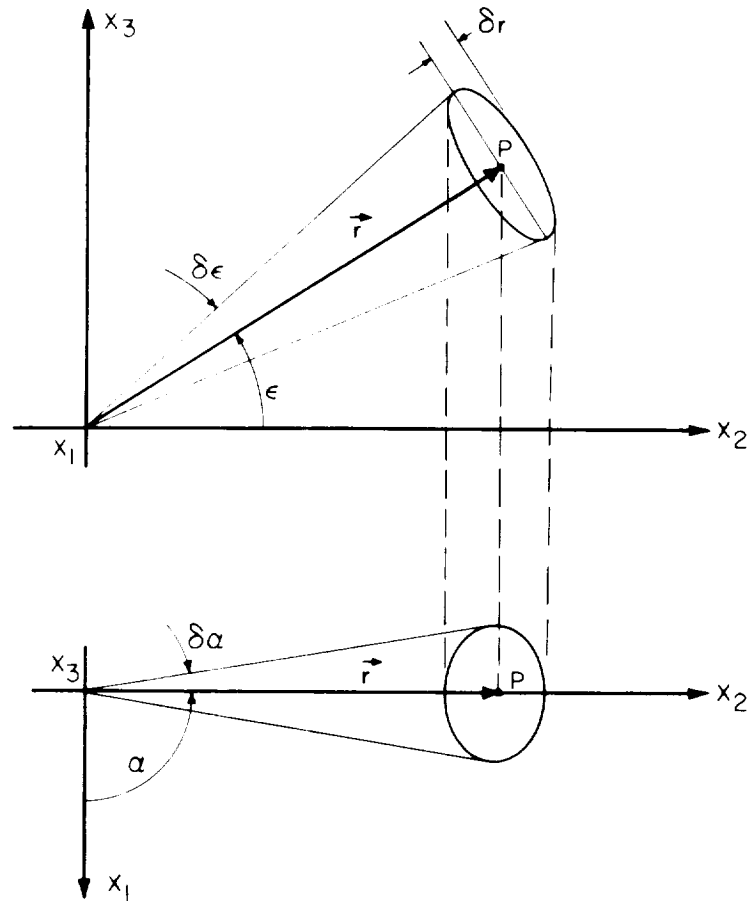


Figure 3 - Schematic of a radar position vector error

GENERAL THEORY OF THE SYSTEM

The point P is determined* by using three stations as shown in Figure 1. In this case no prior known equations of motions are necessary. This is of importance when the system is being used for precise evaluation of the flight path of a vehicle where smoothing times of only 1 or 2 seconds are used. When the equations of motion of a satellite are better known, a least squares solution of many measurements from these three stations will result in a more precise orbit determination.

*For satellites having large slant ranges ($r_i \geq 3,000$ km), 1 station is sufficient for tracking since a large number of measurements can be made, yielding an overdetermined solution for the path.

The position of the point P in space is given (see Figure 1) by

$$r_j = \left[\sum_{i=1}^3 (x_i - x_{ij})^2 \right]^{\frac{1}{2}}, \quad j = 1, 2, 3, \quad (2)$$

where $x_i (i = 1, 2, 3)$ are the vehicle coordinates and $x_{ij} (i = 1, 2, 3 \text{ and } j = 1, 2, 3)$ are the station coordinates. Here r_j is the measured slant range from the j^{th} station to the vehicle.

From Equation 2, which represents 3 equations in the 3 unknown satellite position components x_i , we obtain

$$x_i = f_i(r_j, x_{ij}). \quad (3)$$

Equation 3 requires that the slant range measurements be made at the "same" time at all three stations. In practice this need not be so. The "same" means a time accurate to within ± 1 msec. Such an error in time corresponds only to ± 8 m in satellite position.

A time synchronization around the globe through the use of WWV can be accomplished to within ± 2 msec (References 5, 6, and 7). A synchronization to ± 1 msec between stations separated by approximately 500 to 1000 km as necessary for injection tracking is therefore not difficult.

For reasons of simplicity, assume the following station coordinates as shown in Figure 5:

$$x_{i1}(0, 0, 0); \quad x_{i2}(x_{12}, x_{22}, 0); \quad x_{i3}(0, x_{23}, 0).$$

(This, of course, does not restrict the problem at hand since the local coordinate system can always be assumed as shown in Figure 5 when 3 stations are being used.) The position x_i of the spacecraft is then (from Equations 2 and 3):

$$\left. \begin{aligned} x_1 &= \frac{1}{2x_{12}} \left[r_1^2 - r_2^2 + x_{12}^2 + x_{22}^2 - \frac{x_{22}}{x_{23}} (r_1^2 - r_3^2 + x_{23}^2) \right], \\ x_2 &= \frac{1}{2x_{23}} (r_1^2 - r_3^2 + x_{23}^2), \\ x_3 &= (r_1^2 - x_2^2 - x_{12}^2)^{\frac{1}{2}}. \end{aligned} \right\} \quad (3a)$$

Since the r_j values are measured, Equations 3a can easily be evaluated and the x_i determined.

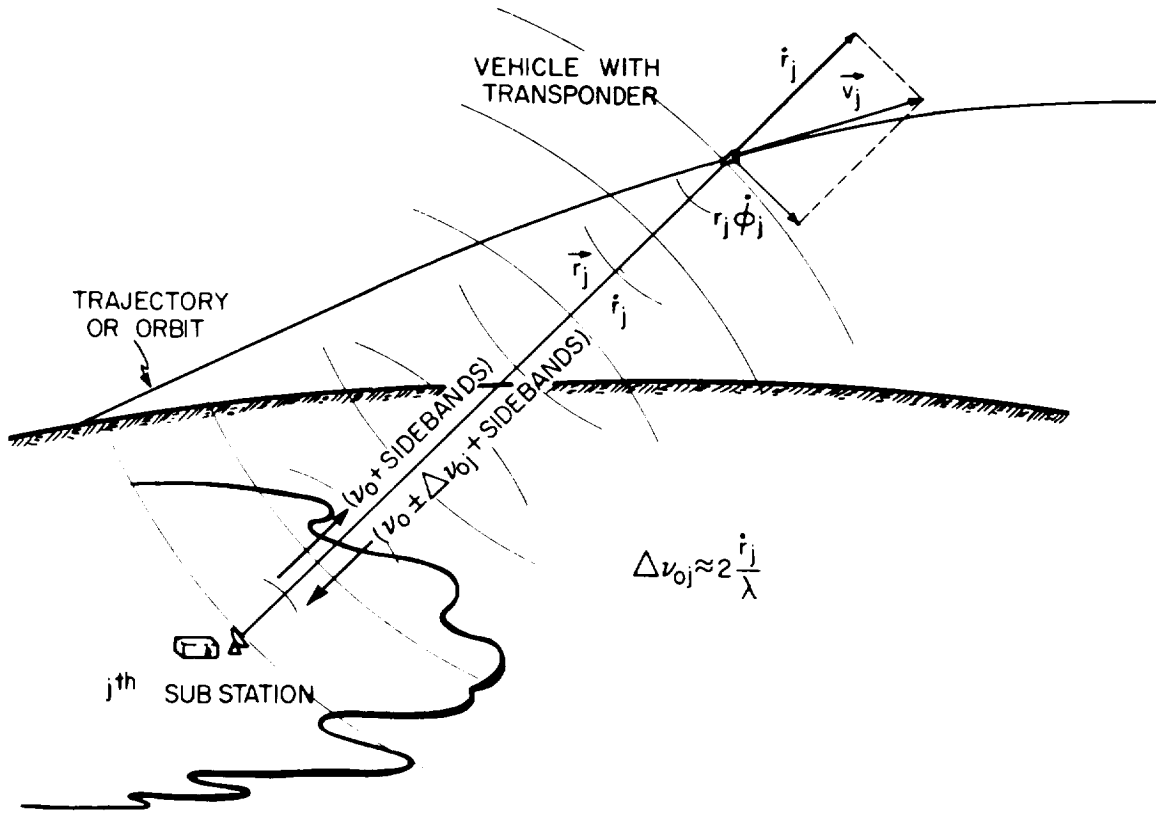


Figure 4 - A substation of a range and range rate system

Differentiating Equations 3a results in

$$\left. \begin{aligned} \dot{x}_1 &= \frac{1}{x_{12}} \left[r_1 \dot{r}_1 \left(1 - \frac{x_{22}}{x_{23}} \right) - r_2 \dot{r}_2 + \frac{x_{22}}{x_{23}} r_3 \dot{r}_3 \right], \\ \dot{x}_2 &= \frac{1}{x_{23}} (r_1 \dot{r}_1 - r_3 \dot{r}_3), \\ \dot{x}_3 &= \frac{1}{x_3} (r_1 \dot{r}_1 - x_2 \dot{x}_2 - x_1 \dot{x}_1). \end{aligned} \right\} \quad (4)$$

Equations 4 give the velocity vector \vec{v} in component form. The values \dot{r}_j are measured by observing the Doppler shift $\Delta \nu_{oj}$ of a frequency ν_0 ; that is, to a first approximation,*

*The relativistic Doppler shift $\left[\frac{1}{2} (v/c)^2 \right]$ corresponding to 1 cps at a frequency of 2Gc ($v = 10$ km/sec) is not considered here.

$$(\Delta\nu_0)_j = \nu_0 \frac{2\dot{r}_j}{c} = \frac{2}{\lambda} \dot{r}_j$$

or

$$\dot{r}_j = \frac{1}{2} \lambda \Delta\nu_{0j} \quad (5)$$

where λ is the wavelength of the frequency used. (The factor of 2 in Equation 5 appears because the vehicle carries a transponder.) Higher terms can of course be included if necessary.

Equations 3a and 4 fully determine the position vector \vec{r} and velocity vector $\vec{v} = \dot{\vec{r}}$. This, of course, was obvious and the emphasis here shall not be directed to Equations 3a and 4.

TRACKING ERRORS

The primary characteristic of a precise tracking system is that the errors in position η_{x_i} and velocity $\eta_{\dot{x}_i}$ are small and their limits known. These errors will be discussed now.

Errors in Position

From Equation 2, the variation of r_j can be obtained to a first order approximation by a simple first order Taylor expansion:

$$\delta r_j = \sum_{i=1}^3 \frac{\partial r_j}{\partial x_i} \delta x_i + \sum_{i=1}^3 \frac{\partial r_j}{\partial x_{ij}} \delta x_{ij} \quad (6)$$

The variational form of Equation 2 as generalized by Equation 6 is given by

$$\delta r_j = \sum_{i=1}^3 a_{ij} (\delta x_i - \delta x_{ij}), \quad (7)$$

where

$$a_{ij} = \left(\frac{x_i - x_{ij}}{r_j} \right) \text{ is the direction cosine of the position vector } \vec{r}_j.$$

Equation 7 can be written for convenience in matrix form as follows:

$$\delta_{(3 \times 1)} = \mathbf{A}_{(3 \times 3)} \delta \mathbf{X}_{(3 \times 1)}, \quad (8)$$

where

$$\mathbf{A} = \begin{bmatrix} a_{11} & a_{21} & a_{31} \\ a_{12} & a_{22} & a_{32} \\ a_{13} & a_{23} & a_{33} \end{bmatrix},$$

$$\delta \mathbf{X} = \begin{bmatrix} \delta x_1 \\ \delta x_2 \\ \delta x_3 \end{bmatrix},$$

and

$$\delta = \begin{bmatrix} \delta r_1 + \sum_{i=1}^3 a_{i1} \delta x_{i1} \\ \delta r_2 + \sum_{i=1}^3 a_{i2} \delta x_{i2} \\ \delta r_3 + \sum_{i=1}^3 a_{i3} \delta x_{i3} \end{bmatrix} = \begin{bmatrix} \delta_1 \\ \delta_2 \\ \delta_3 \end{bmatrix}.$$

From Equation 8 we obtain for the δx_i :

$$\delta \mathbf{X}_{(3 \times 1)} = \mathbf{A}_{(3 \times 3)}^{-1} \delta_{(3 \times 1)}, \quad (9)$$

where

$$\mathbf{A}^{-1} = \begin{bmatrix} a_1 & a_2 & a_3 \\ b_1 & b_2 & b_2 \\ c_1 & c_2 & c_3 \end{bmatrix}$$

is the inverse matrix of \mathbf{A} . If we apply the principle of error propagation, the position errors η_{x_i} then read

$$\left. \begin{aligned} \eta_{x_1} &= \left(\sum_{j=1}^3 a_j^2 T_j \right)^{\frac{1}{2}}, \\ \eta_{x_2} &= \left(\sum_{j=1}^3 b_j^2 T_j \right)^{\frac{1}{2}}, \\ \eta_{x_3} &= \left(\sum_{j=1}^3 c_j^2 T_j \right)^{\frac{1}{2}}, \end{aligned} \right\} \quad (10)$$

where

$$T_j = \frac{1}{N} \delta r_j^2 + \sum_{i=1}^3 a_{ij}^2 \delta x_{ij}^2, \quad (10a)$$

in which N represents the number of measurements taken during a certain time interval Δt . The letter η instead of σ has been chosen for the errors to indicate that the measurements do not obey the normal distribution law. No "smoothing" has been applied to the station position errors δx_{ij} since these are of course constant during all measurements. As can be seen from Equations 10 and 10a, the position errors of the satellite η_{x_i} can not be reduced indefinitely by increasing the smoothing time (that is, increasing N). Only a decrease of the survey errors of the stations δx_{ij} will improve the satellite position errors.

If the time required to make a single measurement ($N = 1$) is designated Δt , then N measurements means a "smoothing time" $\tau = N\Delta t$. One single measurement means actually 3 range and 3 range rate measurements, which determine the position and velocity of a single point in space. In order to get a "feeling" for the errors represented by Equation 10 some examples are given in Figure 5 of a satellite passing over 3 stations in different paths (Cases a, b, c, and d). The detailed graphs from which the composite (total) graphs were made are given in Appendix A. Figures 6 through 9 give, in graphical form, the total position errors $\eta_{x_{tot}}$ as a function of time as the object passes over the 3 stations for Cases a, b, c, and d. Figure 10 gives, in graphical form, the influence of geometry on position errors for Cases a, b, c, and d. The time is also marked in Figure 5 so that a real comparison between the errors and the spacial position of the satellite can be made.

In most cases, one station has no superiority over any other; therefore, it is assumed for the numerical calculation that the errors of these stations δx_{ij} , which are pure survey errors, are equal, that is,

$$\delta x_{ij} = \text{constant} = \delta x_s.$$

TN D-1178

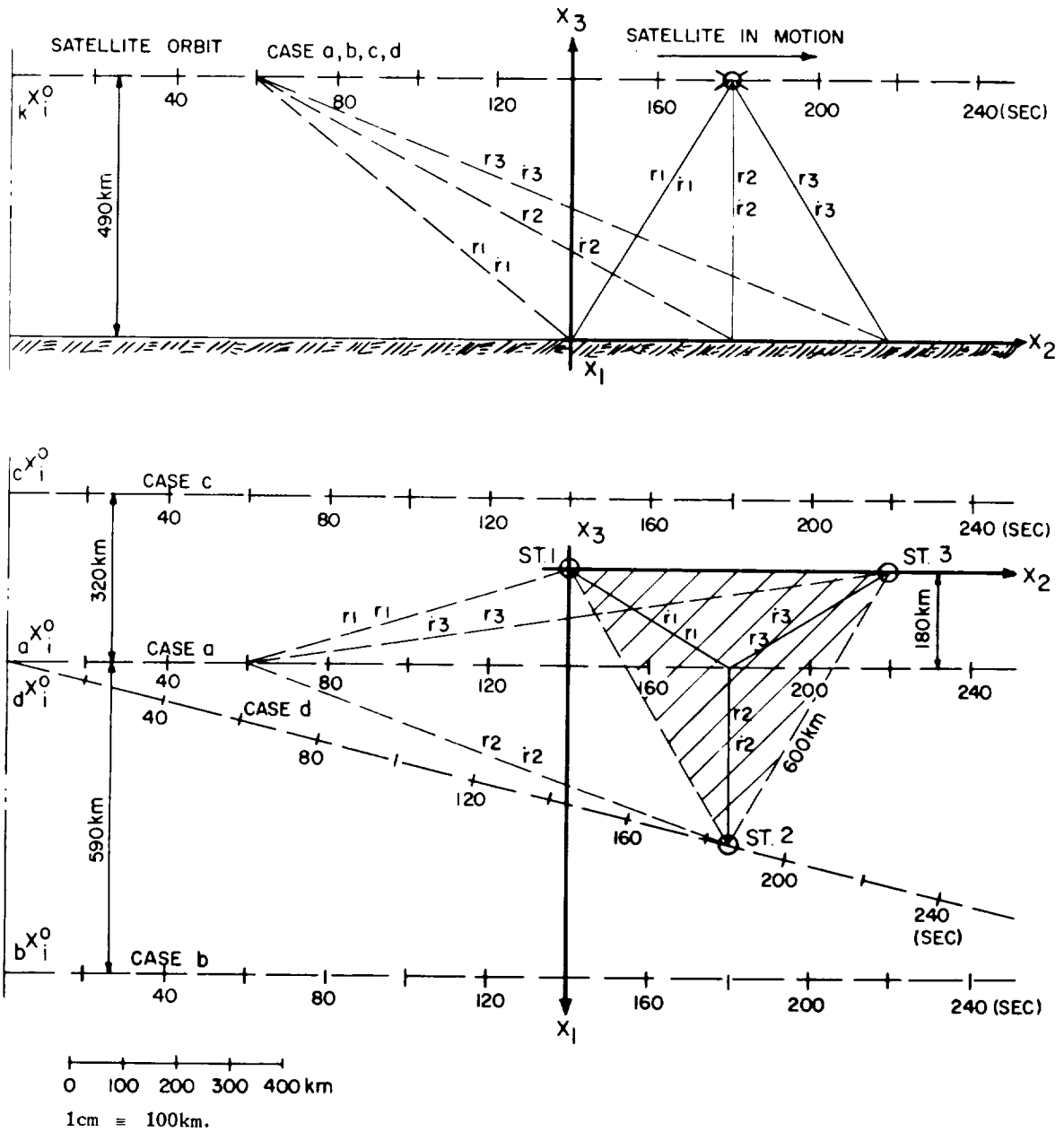


Figure 5 - The three-stations solution for the $(r + \dot{r})$ system

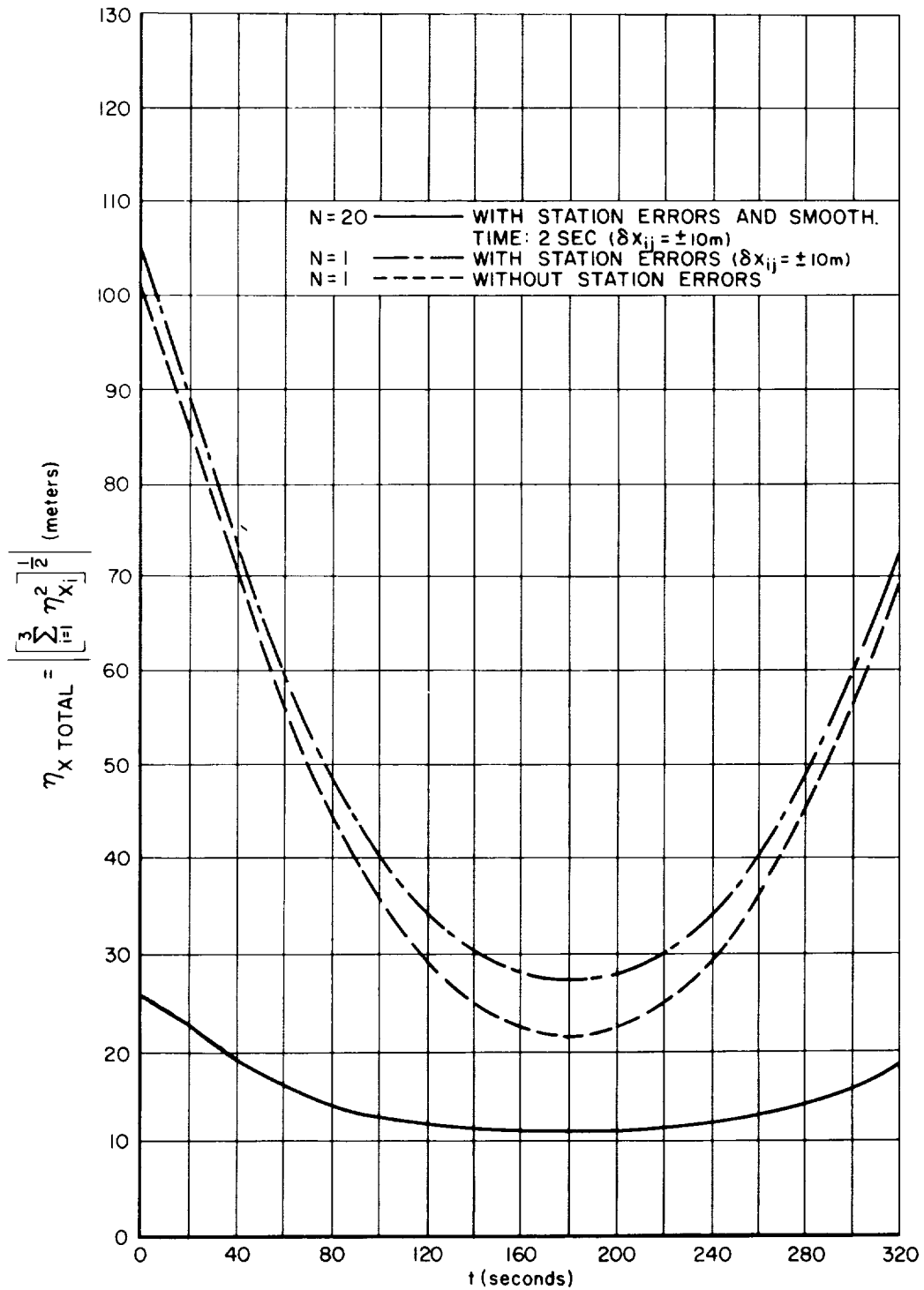


Figure 6 - Total satellite position errors for Case a shown in Figure 5 (also see Appendix A); $\delta_r = \pm 10$ meters

TN D-1178

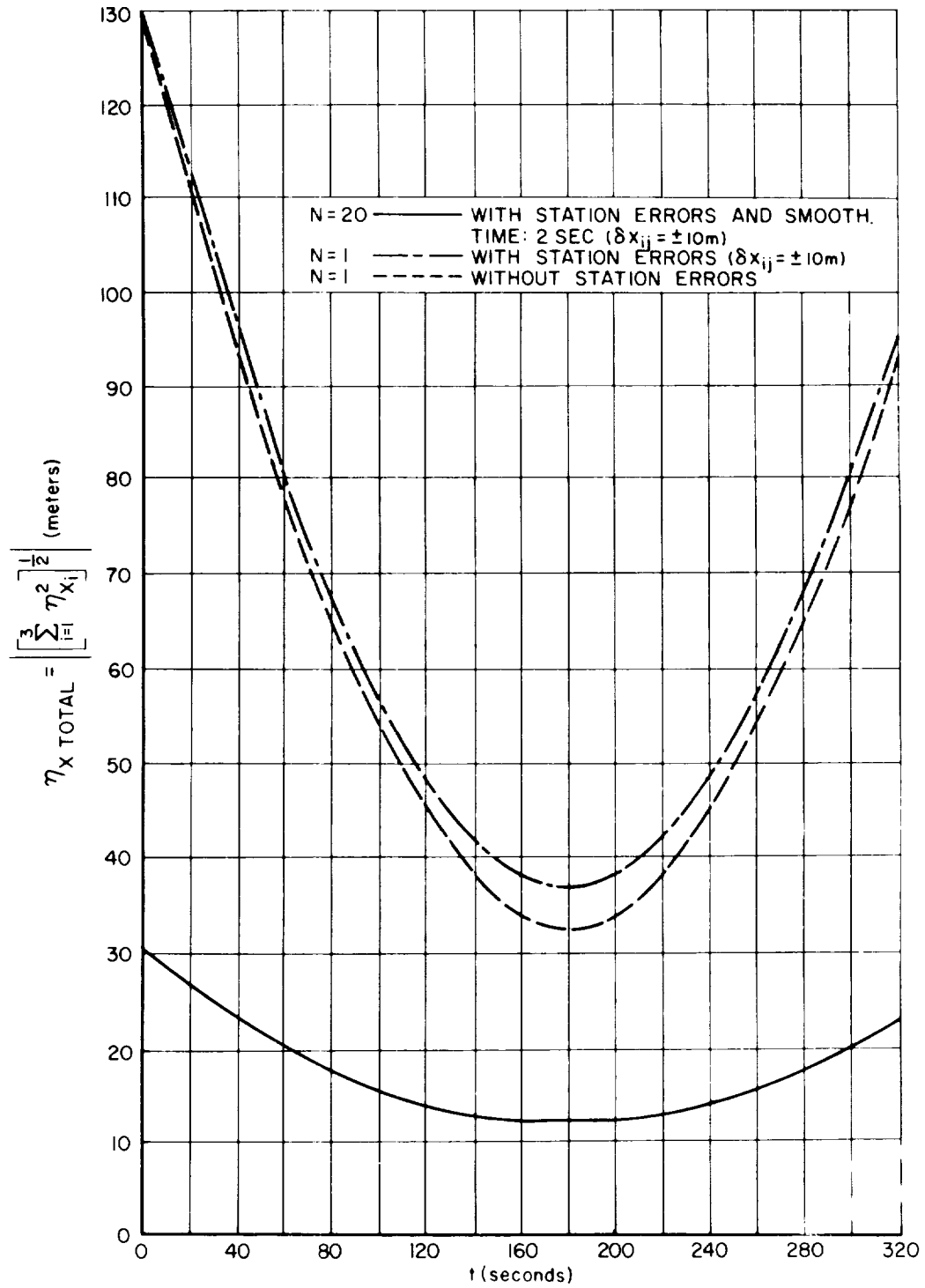


Figure 7 - Total satellite position errors for Case b shown in Figure 5 (also see Appendix A); $\delta r = \pm 10$ meters

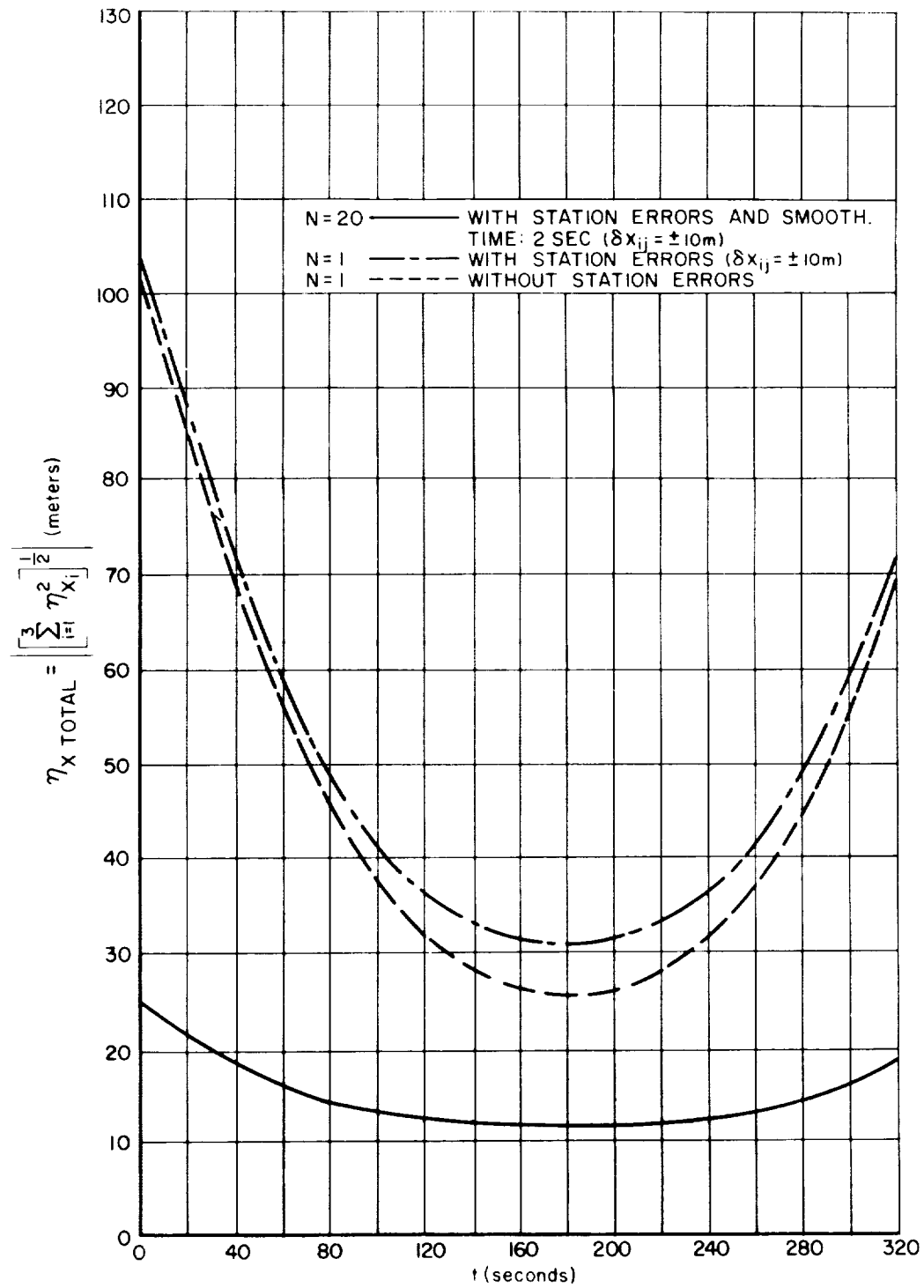


Figure 8 - Total satellite position errors for Case c shown in Figure 5 (also see Appendix A); $\delta r = \pm 10$ meters

D-1110

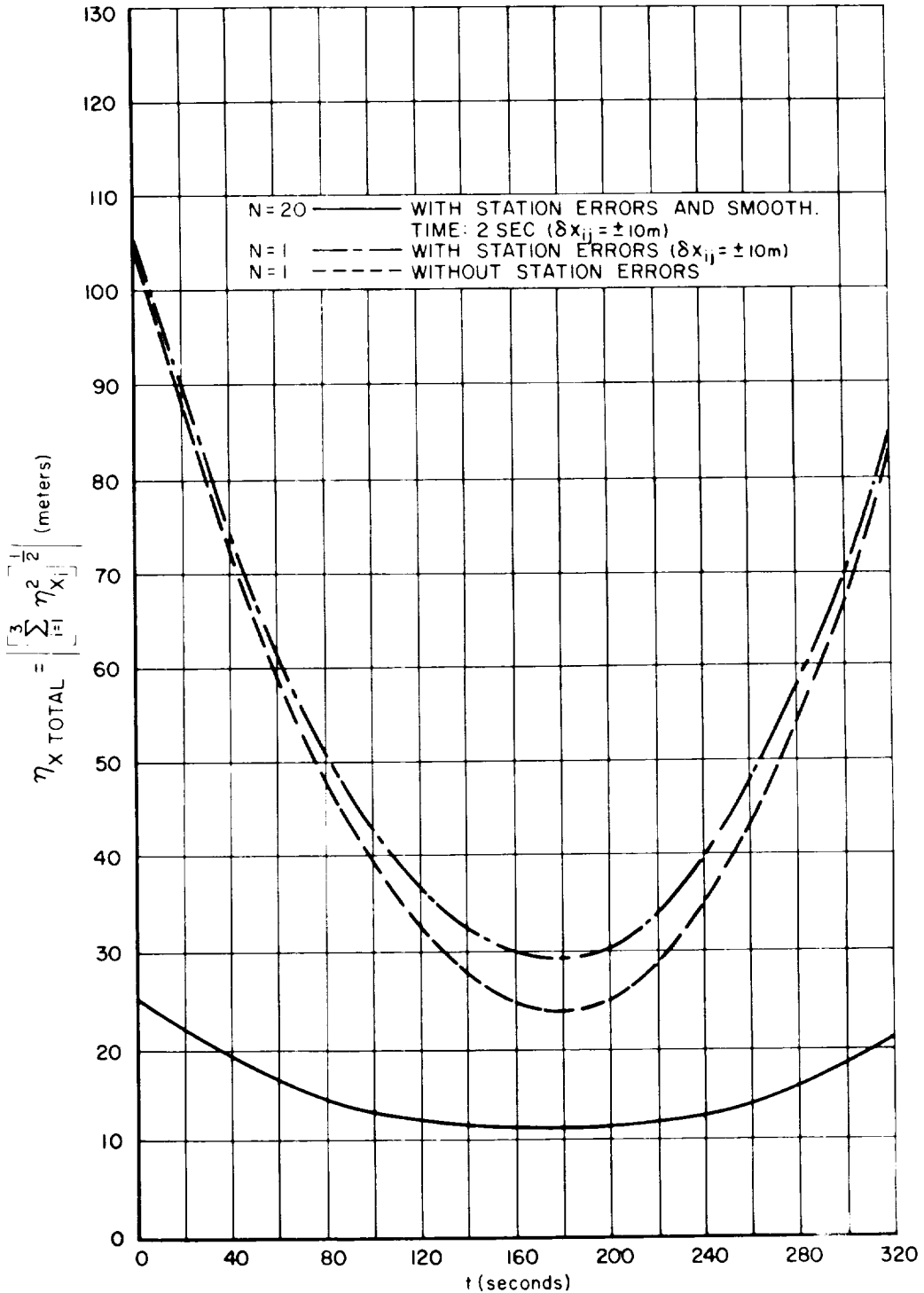


Figure 9 - Total satellite position errors for Case d shown in Figure 5 (also see Appendix A); $\delta r = \pm 10$ meters

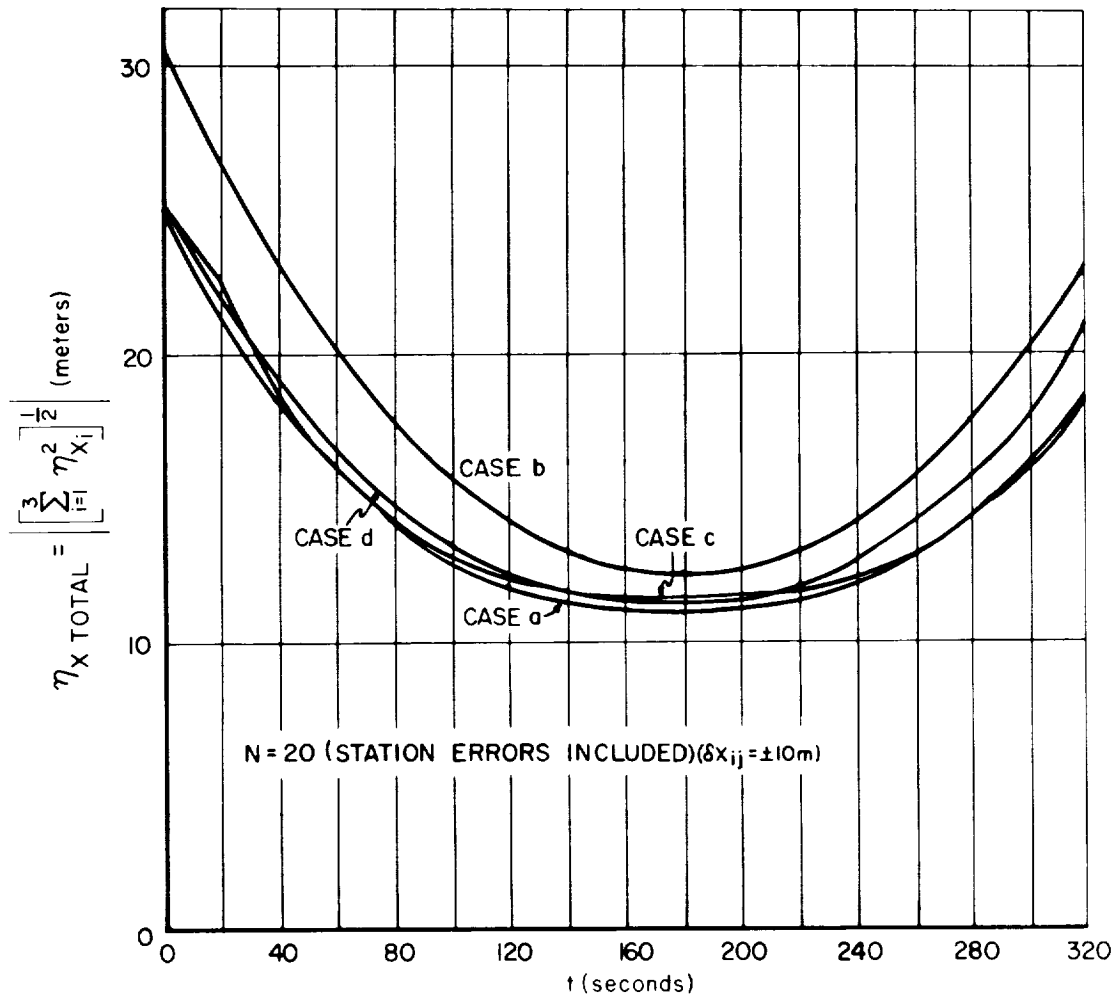


Figure 10 - Influence of geometry on the total satellite position errors shown in Figure 5; $\delta r = \pm 10$ meters

In this report the following measurement errors for a single measurement during a time Δt have been used:

$$\delta r_j = \pm 10 \text{ m},$$

$$i = j = 1, 2, 3$$

$$\delta x_s = \delta x_{ij} = \pm 10 \text{ m},$$

with no smoothing time ($N = 1$ or $\tau = \Delta t = 0.1$ sec) and with smoothing time ($N = 20$ or

$\tau = 2$ sec). Since in this treatment the δx_{ij} have been assumed equal, the expression for the T_j is simplified to

$$T_j = \frac{1}{N} \delta r_j^2 + \delta x_s^2 \quad (10b)$$

because

$$\sum_{i=1}^3 \alpha_{ij}^2 = 1.$$

Errors in Velocity

The velocity components \dot{x}_i of a satellite can be found from Equation 2 by differentiation with respect to time:

$$\dot{r}_j = \frac{1}{r_j} \sum_{i=1}^3 \dot{x}_i (x_i - x_{ij}),$$

or

$$\dot{r}_j = \sum_{i=1}^3 \alpha_{ij} \dot{x}_i. \quad (11)$$

The variation of \dot{r}_j can be obtained in the manner as generalized by Equation 6 resulting in:

$$\delta \dot{r}_j = \frac{1}{r_j} \sum_{i=1}^3 x_i (\delta x_i - \alpha_{ij} \delta r_j - \delta x_{ij}) + \sum_{i=1}^3 \alpha_{ij} \delta \dot{x}_i. \quad (12)$$

Again, Equation 12 can be expressed in matrix form as:

$$\Gamma_{(3 \times 1)} = A_{(3 \times 3)} \cdot \delta \dot{X}_{(3 \times 1)}, \quad (13)$$

where the Γ -matrix reads, from Equations 12 and 13:

$$\Gamma = \begin{bmatrix} \delta \dot{r}_1 - \frac{1}{r_1} \sum_{i=1}^3 \dot{x}_i (\delta x_i - a_{i1} \delta r_1 - \delta x_{i1}) \\ \delta \dot{r}_2 - \frac{1}{r_2} \sum_{i=1}^3 \dot{x}_i (\delta x_i - a_{i2} \delta r_2 - \delta x_{i2}) \\ \delta \dot{r}_3 - \frac{1}{r_3} \sum_{i=1}^3 \dot{x}_i (\delta x_i - a_{i3} \delta r_3 - \delta x_{i3}) \end{bmatrix} = \begin{bmatrix} \gamma_1 \\ \gamma_2 \\ \gamma_3 \end{bmatrix}.$$

Equation 13 can now be solved for the velocity variations $\delta \dot{x}_i$, that is:

$$\delta \dot{\mathbf{X}}_{(3 \times 1)} = \mathbf{A}_{(3 \times 3)}^{-1} \Gamma_{(3 \times 1)}, \quad (13a)$$

where

$$\delta \dot{\mathbf{X}} = \begin{bmatrix} \delta \dot{x}_1 \\ \delta \dot{x}_2 \\ \delta \dot{x}_3 \end{bmatrix}$$

and

$$\delta \dot{x}_1 = \sum_{i=1}^3 a_i \gamma_i,$$

$$\delta \dot{x}_2 = \sum_{i=1}^3 b_i \gamma_i,$$

$$\delta \dot{x}_3 = \sum_{i=1}^3 c_i \gamma_i.$$

By using the principle of error propagation again, we obtain from Equations 13 and 13a

for the velocity errors $\eta_{\dot{x}_i}$:

$$\left. \begin{aligned} \eta_{\dot{x}_1} &= \left(\sum_{j=1}^3 a_j^2 S_j \right)^{\frac{1}{2}}, \\ \eta_{\dot{x}_2} &= \left(\sum_{j=1}^3 b_j^2 S_j \right)^{\frac{1}{2}}, \\ \eta_{\dot{x}_3} &= \left(\sum_{j=1}^3 c_j^2 S_j \right)^{\frac{1}{2}}, \end{aligned} \right\} \quad (14)$$

where

$$S_j = \frac{1}{N} \delta \dot{r}_j^2 + \frac{1}{N} \frac{1}{r_j^2} \sum_{i=1}^3 \dot{x}_i^2 \left(\delta x_{ij}^2 + a_{ij}^2 \delta r_j^2 \right) + \frac{1}{r_j^2} \sum_{i=1}^3 \dot{x}_i^2 \delta x_{ij}^2. \quad (14a)$$

Again N represents the number of measurements taken during a time τ . Equation 14a shows clearly (similarly to Equation 10a) that the velocity errors $\eta_{\dot{x}_i}$ depend largely on the station position errors δx_{ij} which are, of course, constant and therefore not subject to statistics expressed by N . Only a good survey of the stations can ever reduce the errors $\eta_{\dot{x}_i}$ unless the slant ranges r_j are large.

These equations giving the velocity error components $\eta_{\dot{x}_i}$ can be evaluated since all the quantities which appear on the right side of Equations 14 are measured and known. For the variations δx_{ij} of the satellite, the rms values $\eta_{x_{ij}}$ of a single observation ($N = 1$ in Equation 10) have to be used.

In order to get an idea of these tracking velocity errors, the values $\eta_{\dot{x}_i}$, are presented in Figures 11 through 14 in graphical form for the Cases a, b, c and d shown in Figure 5. The detailed groups from which the composite (total) graphs were made are given in Appendix B. Figure 15 gives, in graphical form, the influence of geometry on velocity errors for the four cases.

The following measuring errors for the radial velocities have been assumed in this report:

$$\delta \dot{r}_j = \pm 0.2 \text{ m/sec}, \quad j = 1, 2, 3.$$

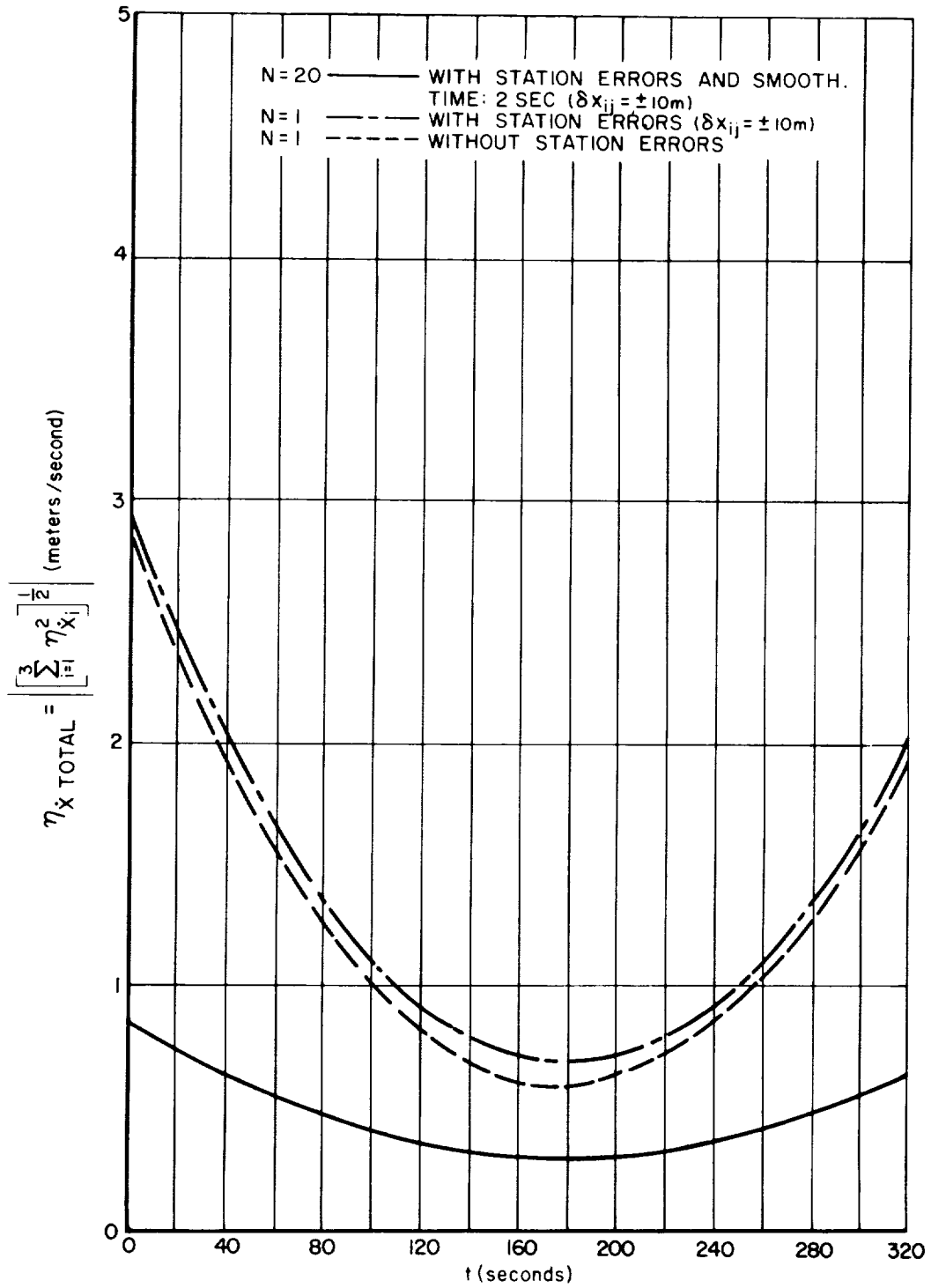


Figure 11 - Total satellite velocity errors for Case a shown in Figure 5 (see also Appendix B);
 $\delta r = \pm 10$ meters, $\delta \dot{r} = \pm 0.2$ meter/second

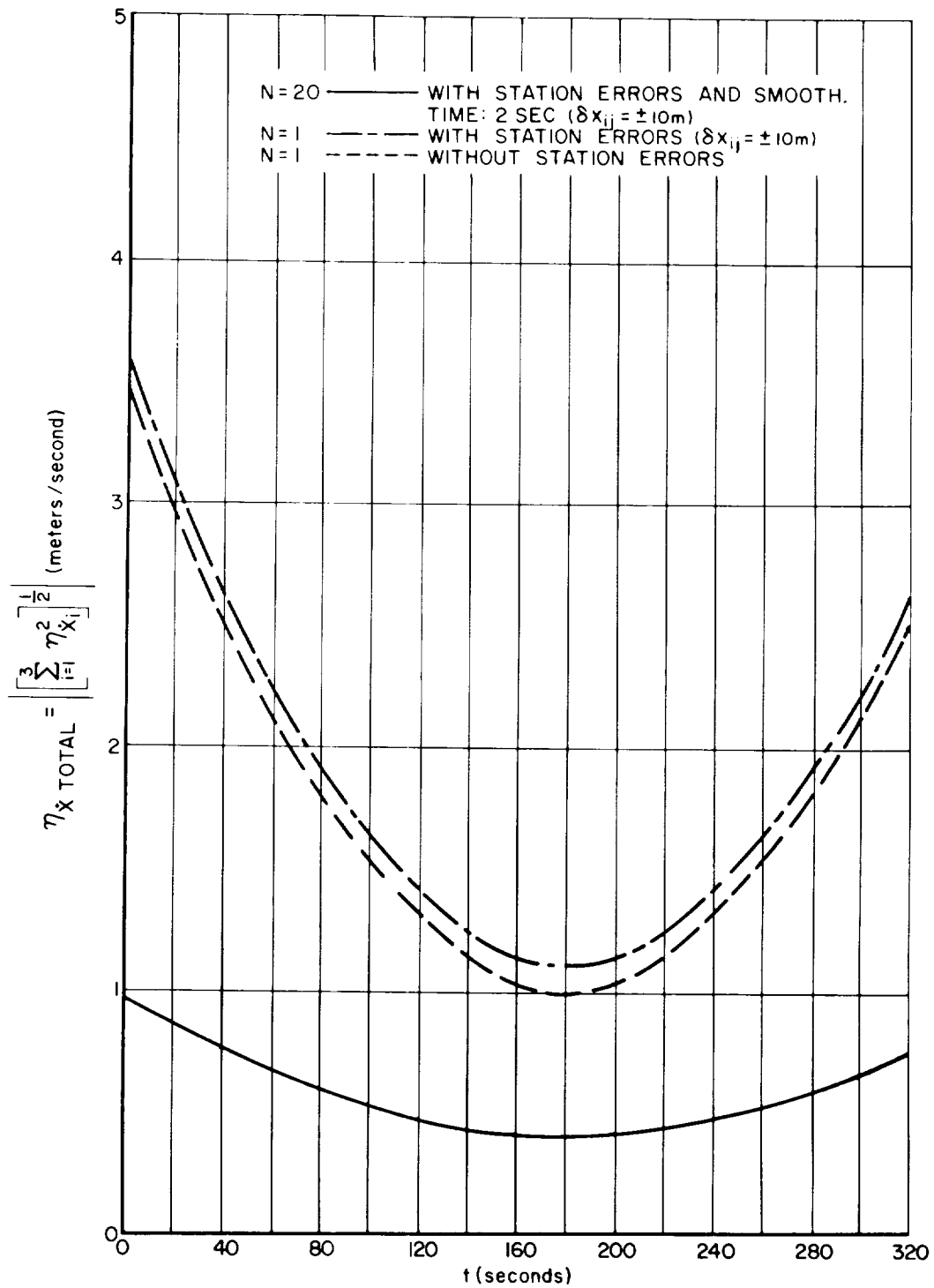


Figure 12 - Total satellite velocity errors for Case b shown in Figure 5 (see also Appendix B);
 $\delta r = \pm 10$ meters, $\delta \dot{r} = \pm 0.2$ meter/second

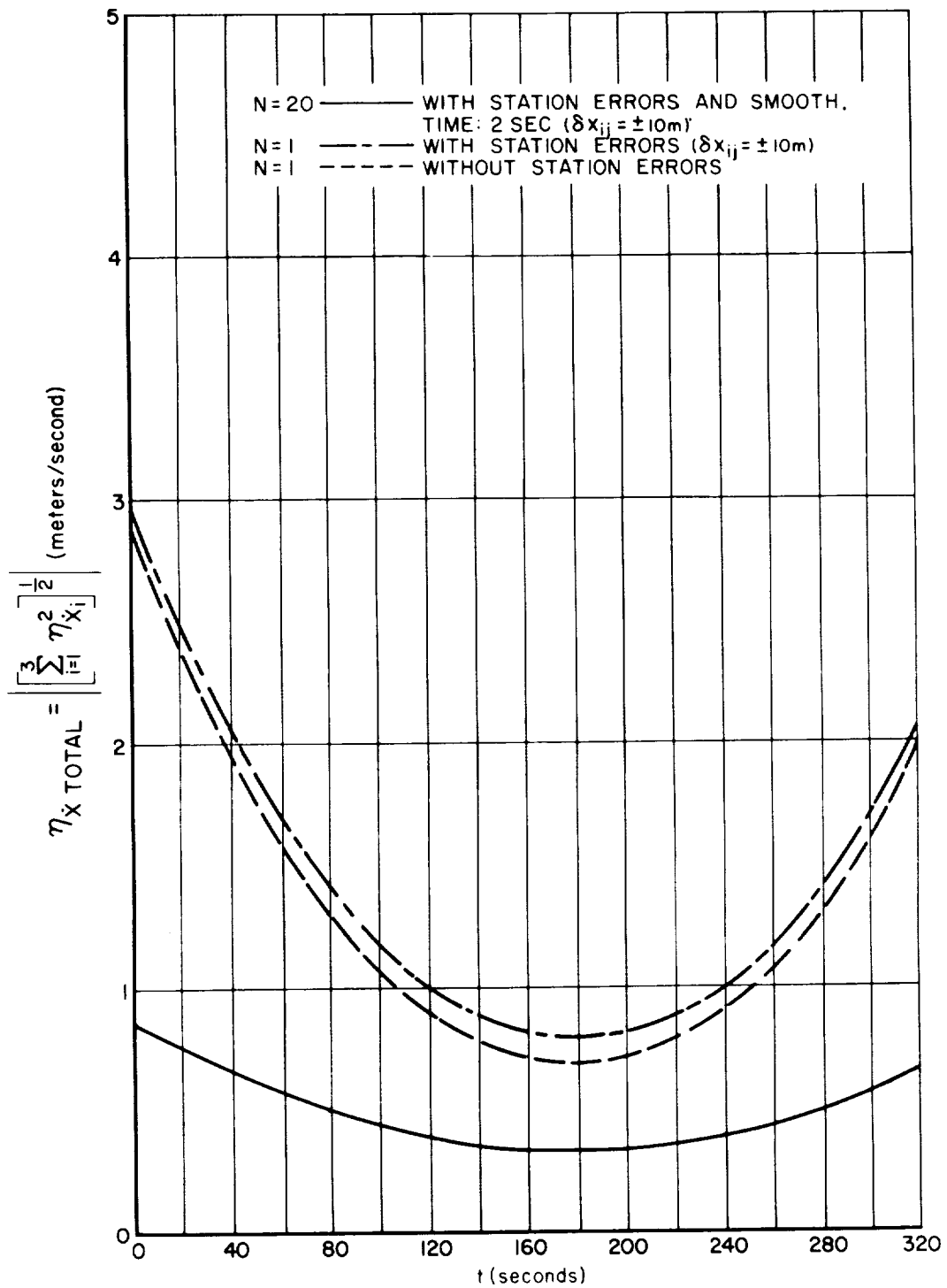


Figure 13 - Total satellite velocity errors for Case c shown in Figure 5 (see also Appendix B);
 $\delta r = \pm 10$ meters, $\delta \dot{r} = \pm 0.2$ meter/second

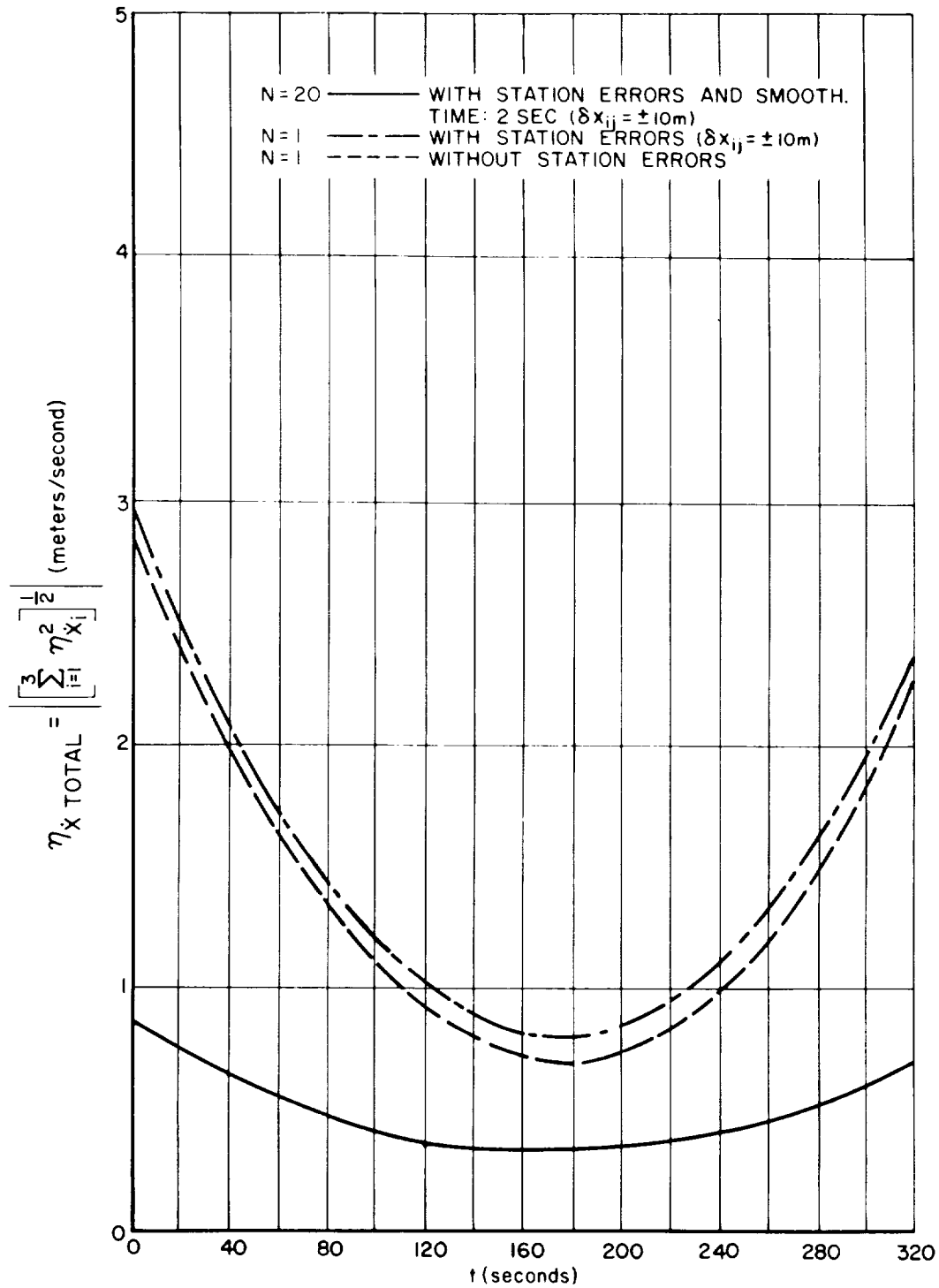


Figure 14 - Total satellite velocity errors for Case d shown in Figure 5 (see also Appendix B); $\delta r = \pm 10$ meters, $\delta \dot{r} = \pm 0.2$ meter/second

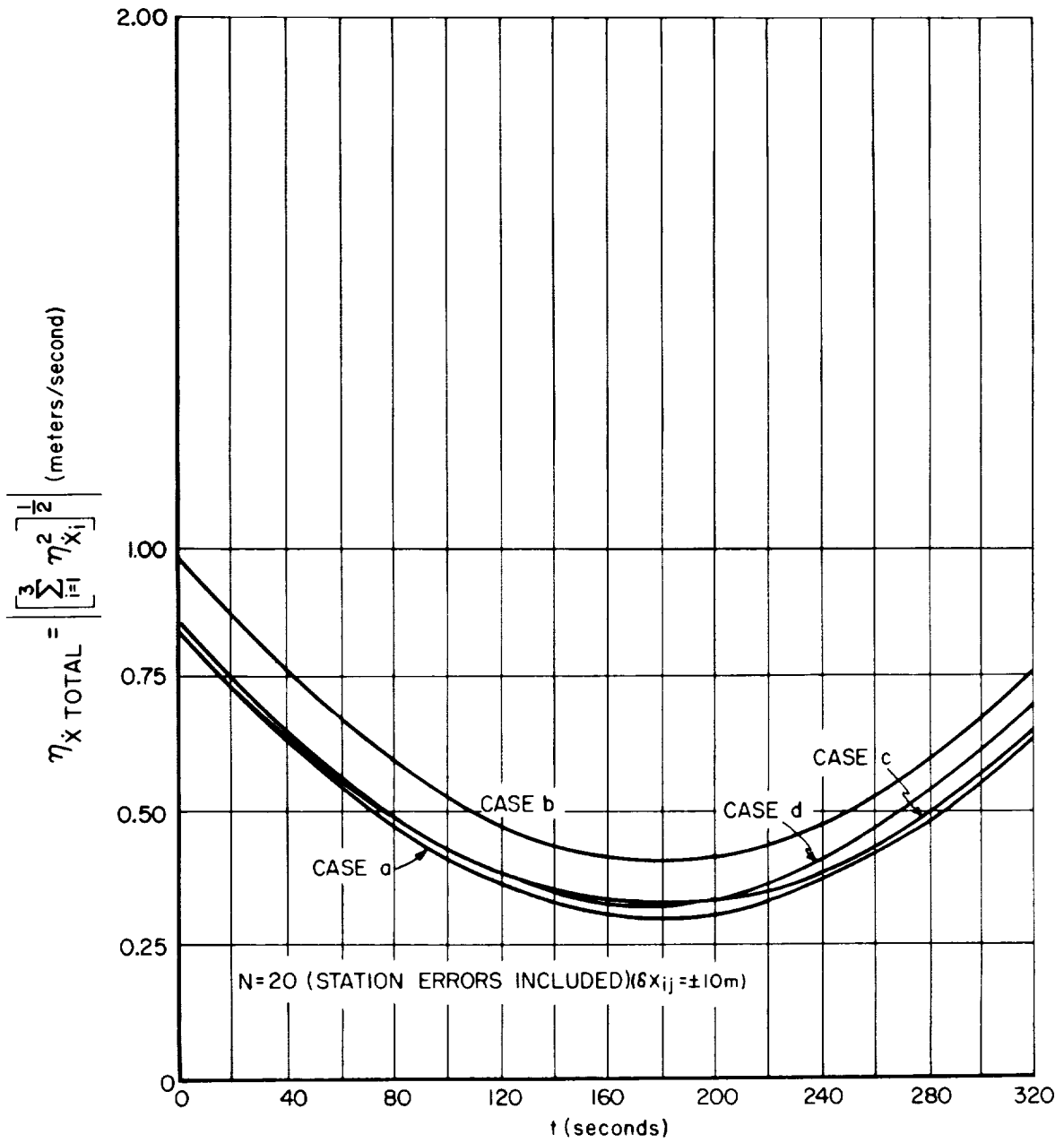


Figure 15 - Influence of geometry on total satellite velocity errors;
 $\delta r = \pm 10$ meters, $\delta \dot{r} = \pm 0.2$ meter/second

If a frequency of, say, 2 Gc ($\lambda = 15$ cm) is used, the above error corresponds to a Doppler error (from Equation 5) of

$$\delta \Delta \nu_{0j} = \frac{2}{\lambda} \delta \dot{r}_j = \frac{2}{0.15} \times 0.2 \approx 3 \text{ cps,}$$

which is actually a very large one.

For large slant ranges r_j , the velocity errors depend only on the uncertainty $\delta \dot{r}_j$ in the measurement of \dot{r}_j as can be seen from Equations 14a. This is the case for

$$\frac{1}{N} \delta \dot{r}_j^2 \gg \frac{1}{N} \frac{1}{r_j^2} \sum_{i=1}^3 \dot{x}_i^2 \left(\delta x_i^2 + a_{ij}^2 \delta r_j^2 \right) + \frac{1}{r_j^2} \sum_{i=1}^3 \dot{x}_i^2 \delta x_{ij}^2. \quad (15)$$

For the worst condition, namely $N = 1$, Equation 15 is satisfied for slant ranges $r_j \geq 8000$ km. For these cases, the velocity errors are given from Equations 14 and 15 by:

$$\left. \begin{aligned} \eta_{\dot{x}_1} &= \left(\frac{1}{N} \sum_{i=1}^3 a_i^2 \delta \dot{r}_i^2 \right)^{\frac{1}{2}}, \\ \eta_{\dot{x}_2} &= \left(\frac{1}{N} \sum_{i=1}^3 b_i^2 \delta \dot{r}_i^2 \right)^{\frac{1}{2}}, \\ \eta_{\dot{x}_3} &= \left(\frac{1}{N} \sum_{i=1}^3 c_i^2 \delta \dot{r}_i^2 \right)^{\frac{1}{2}}. \end{aligned} \right\} \quad (16)$$

In using 3 stations for extremely large distances, care must be taken in applying Equation 16 because the matrix A becomes ill-conditioned, since the elements of the the inverted matrix A^{-1} , namely a_i , b_i , and c_i , are very uncertain under such conditions.

In order to demonstrate the usefulness of the error equations in this simple form as presented here, a further example is worked out in the following.

Assume the problem is to determine what influence the uncertainties of the ship positions $\delta \dot{x}_{ij}$ have when ships are used as tracking stations. In brief, what are the errors in position η_{x_i} and velocity $\eta_{\dot{x}_i}$ of a spacecraft in this case?

In order to make use of the graphs presented here, the previous position errors δx_{ij} are related to the position errors of the ships $\delta \dot{x}_{ij}$ that is: $\delta \dot{x}_{ij} = k_i \delta x_{ij}$.

Equation 10a can then be simplified to

$$\sigma_j^2 \doteq k^2 \sum_{i=1}^3 \alpha_{ij}^2 \delta x_{ij}^2 \quad (10c)$$

since

$$\delta r_j^2 \ll k_i^2 \delta x_{ij}^2 \text{ with } k_i = k \geq 10.$$

Equation (10c) introduced into (10) results in

$$\eta'_{x_i} \doteq k \eta_{x_i} \quad i = 1, 2, 3. \quad (10d)$$

This means that the errors of spacecraft position η'_{x_i} when ships are used are k times the previous errors (when land based stations are used). All the graphs (Figures 5 - 9) presented here are therefore useful and have only to be multiplied by k . As an example, δx_{ij} was previously assumed to be ± 10 meters for land stations. In order to obtain uncertainties in the ships position of, say, $\delta x_{1j} = \delta x_{2j} = \pm 500$ m (1/3 statute miles) and $\delta x_{3j} = \pm 100$ m (300 ft) the values of $k_1 = k_2 = 50$ and $k_3 = 10$ have to be chosen ($\delta'_{x_{ij}} = k_i \delta x_{ij}$).

The same holds of course for the velocity errors $\eta'_{\dot{x}_i}$.

Equation (14a) reduces then to

$$\delta'_j \doteq k^2 S_j$$

and

$$\eta'_{\dot{x}_i} \doteq k \eta_{\dot{x}_i} \quad (14b)$$

Equation (14b) shows very clear that the uncertainty $\delta'_{x_{ij}}$ in station (ships) position has a large effect on the velocity error of the spacecraft to be tracked.

Also here, the curves shown in Figures 10 - 14 can be used when multiplied by the proper values of k .

It should be noted that smoothing does not help at all in this case since, as was mentioned earlier, the station position uncertainties are constant during a measurement period.

Equations 10d and 14b hold of course in principle for all other tracking systems such as radars, Doppler systems, and so on.

In conclusion it can therefore be said that only accurate station positions will give small position and velocity errors of the object being tracked. This situation becomes less critical for the velocity errors when the slant ranges r_j are large (say 8000 km or larger) as can be seen from Equation 14a.

The foregoing analysis is, of course, not restricted to a local cartesian coordinate system. The same error equations, that is, Equations 10 and 14, can be applied to any type of cartesian coordinate system. In Figure 2, however, the origin of the coordinate system is located at the center of the earth; therefore, Equations 3a and 4 are not applicable in this case. Similar equations can be worked out for this case in a quite elementary manner for the position x_i and velocity \dot{x}_i . Since the position vectors $\vec{s}_j = (x_i)$ of the stations and their motion with time (earth rotation) are known, Equations 10 and 14 can be used generally when the values r_j and \dot{r}_j are known by measurements.

Influence of the Troposphere and Ionosphere

The influence of the troposphere and ionosphere is not treated in this report simply because its influence on range and range rate is small at a frequency of 2 Gc and can be mathematically corrected by using standard profiles. The deviations due to the uncertainties and variations of these profiles for elevation angles $\epsilon \geq 5^\circ$ are certainly smaller than the errors δr_j and $\delta \dot{r}_j$ assumed before. For instance, as S. M. Harris (Reference 8) points out for a satellite at an elevation angle of $\epsilon = 30^\circ$ and a frequency of 200 Mc, the remaining error in range is only 16 m. At 2000 Mc this error would be in the order of 0.16 m and therefore can certainly be neglected (References 9, 10, and 11).

CONCLUSIONS

We have seen, using a simplified description, that the errors in position and velocity, η_{x_i} and $\eta_{\dot{x}_i}$, are indeed very small when very moderate measuring accuracies δr_j and $\delta \dot{r}_j$ of the only measured quantities r_j and \dot{r}_j are used, as well as a very short smoothing time τ . Very poor conditions, as far as errors for this system are concerned, have been presented in graphical form (Figures 6 - 15). These poor conditions also take into account a time synchronization error between the station of about ± 1 msec (corresponding to an error of ± 8 m in position). In brief, no severe time synchronization is necessary at all. This, of course, simplifies the system requirements.

It has been further demonstrated that the geometry (position of satellite with respect to the ground station) does not have too significant an influence on the position and velocity errors (see Figures 10 and 15). This is particularly important where such a system of three or more ground stations is used to track the injection or re-entry of lunar or planetary transfer vehicles. A change in launch time or launch azimuth, which in turn will change the trajectory over the stations (Figure 5), does not therefore harm injection tracking. (A report is being prepared on the application of the $(r + \dot{r})$ system for tracking satellites and spacecraft such as Apollo. Injection, midcourse, and re-entry tracking will be covered in particular.)

Further, it has been shown that the uncertainty in the station position greatly influences the errors in position and velocity of a spacecraft. When ships which have position uncertainties of the order of say ± 500 m (1/3 statute miles) are used, errors in satellite position of approximately ± 500 m and velocity errors of ± 2 m/sec result. [A multiplying factor $k = 50$ has to be used for this particular example

$$\delta x_{ij} = \pm 500 \text{ m} = 50 (\pm 10) \text{ m} .]$$

It should also be noted here that hardware for such a system as described has actually been built at the Goddard Space Flight Center. This system operates at a frequency of 250 Mc (because of availability of equipment) and has been tested by using a calibration airplane. A preliminary summarizing report on this development and test (Reference 12) shows that sophisticated equipment on the ground or in the vehicle is not necessary. Tracking to lunar distances, for instance, can be accomplished by using a 1.5-meter (5-foot) dish on the vehicle which radiates 1 watt, and a 10-meter (30-foot) dish on the ground.

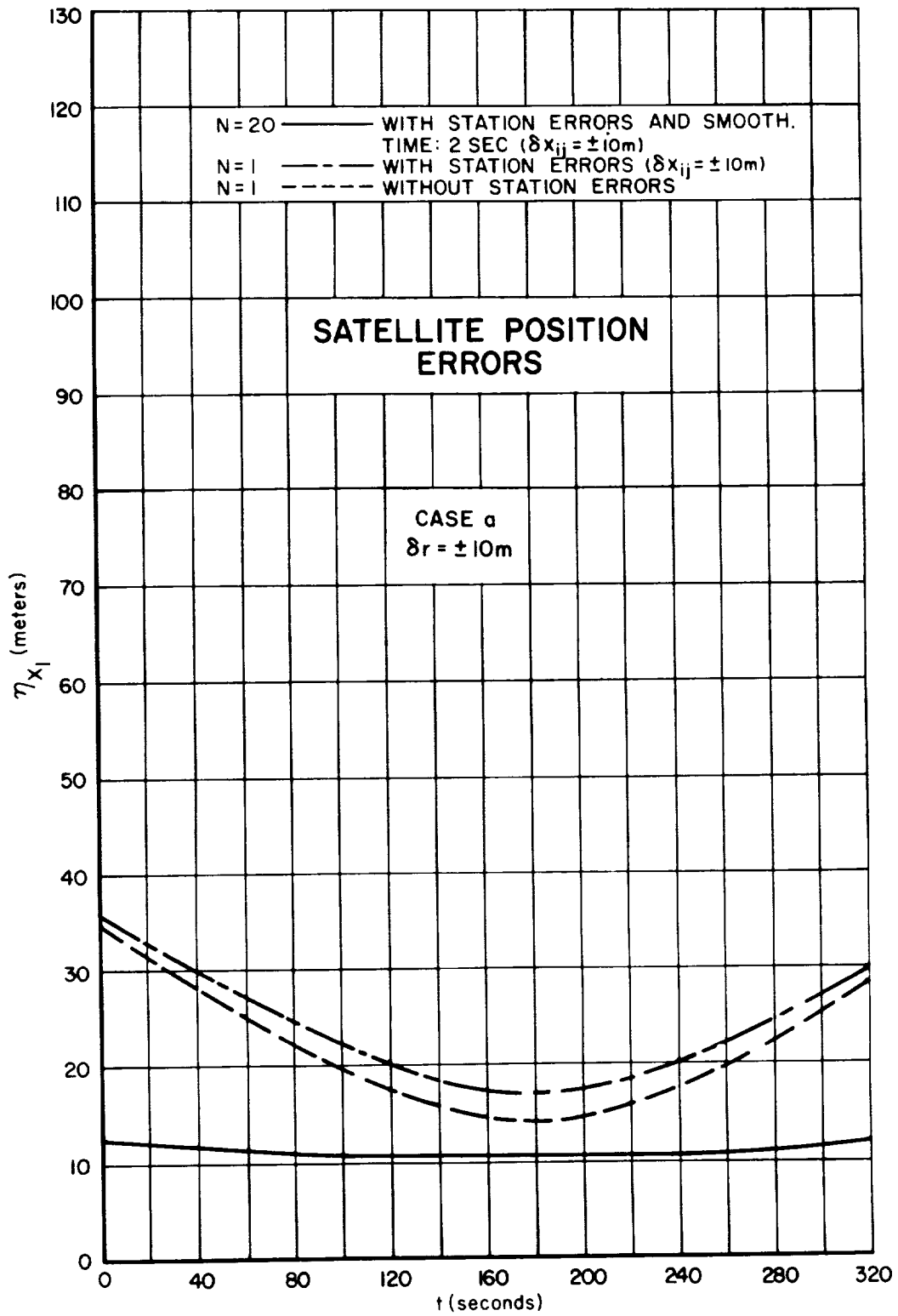
The Goddard Space Flight Center is procuring an $(r + \dot{r})$ system which will operate at a frequency between 1 and 2 Gc. This system will be used by NASA for the Communication Satellite and for the Orbiting Geophysical Observatory. Plans using an $(r + \dot{r})$ system for support of manned space flight are being presently worked out.

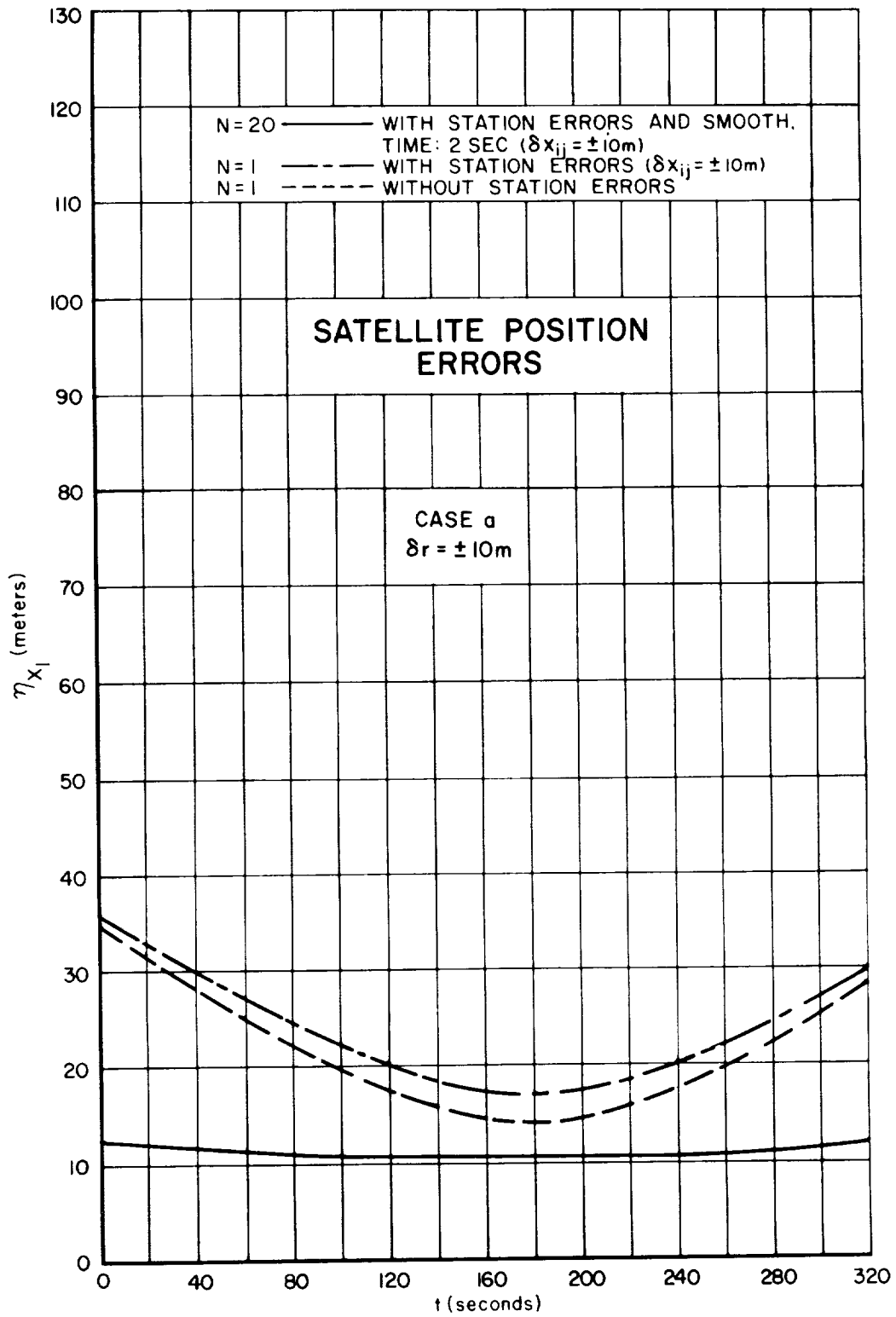
ACKNOWLEDGMENTS

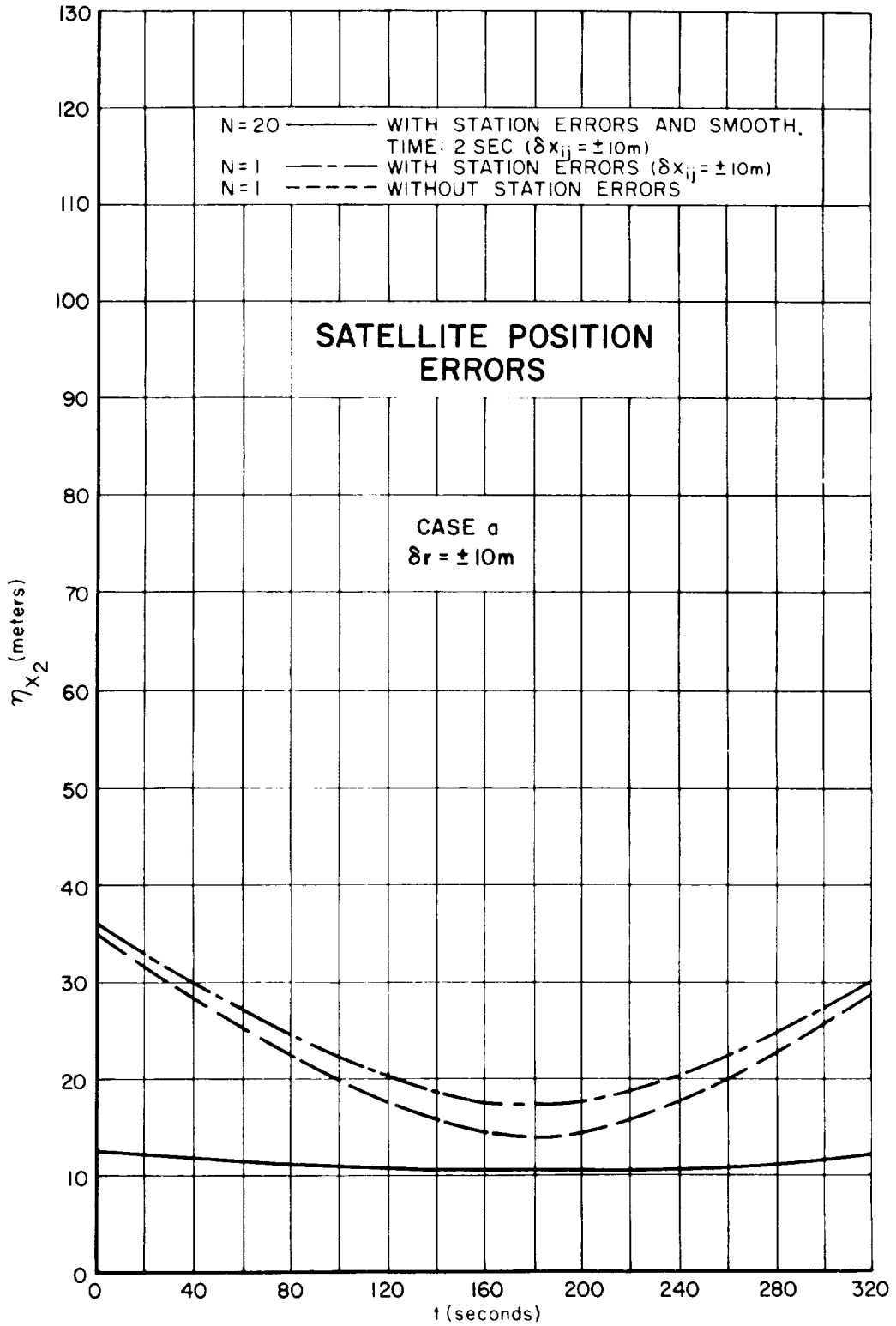
The author wishes to acknowledge the help of Mr. T. Jones in the numerical evaluation of the derived equations.

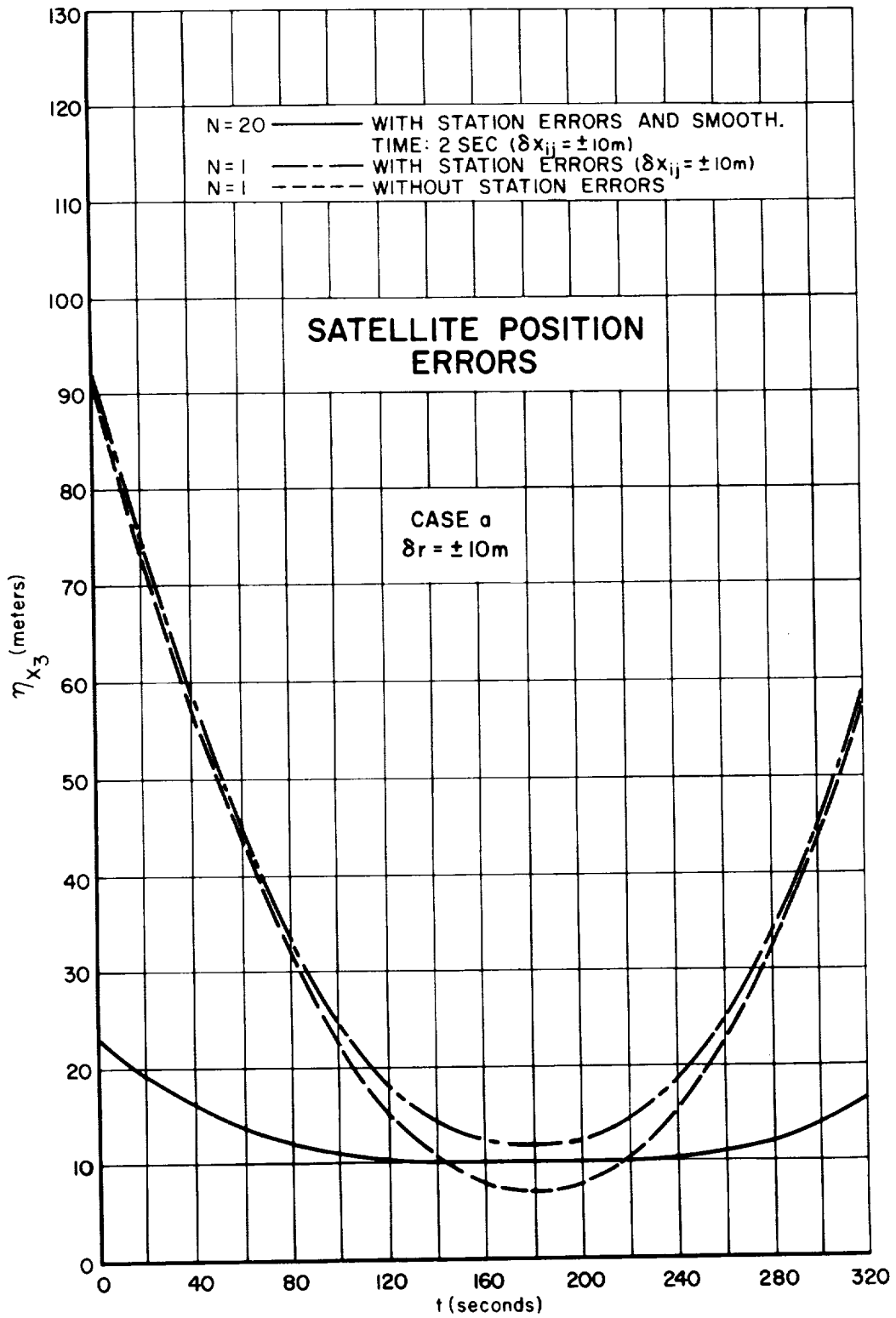
REFERENCES

1. Richardson, J. M., International Scientific Radio Union, 13th General Assembly, London (1960) Commission
2. Froome, K. D., "Investigation of a New Form of Micro-Wave Interferometer for Determining the Velocity of Electromagnetic Waves," Proc. Roy. Soc. London 223A(1153):195-215, April 22, 1954
3. Pearson, K., "Evaluation of the AN/FPS-16 (System Nr. 1) at White Sands Missile Range," U. S. Army Signal Missile Supply Agency Tech. Memo No. 606, February 1959
4. Barton, D. K., File Memo 50.12b, 1 April 1959, R.C.A. Missile and Surface Radar Department, Moorestown, New Jersey
5. "Standard Frequencies and Time Signals WWV and WWVII," Letter Circular LC 1023, Nat. Bur. Standards, Boulder Laboratories, June 1956
6. National Physical Laboratory, "Standard-Frequency Transmissions, Changes in the MSF Standard," Electronic and Radio Eng. 36(3):117-118, March 1959
7. Morgan, A. H., "Precise Time Synchronization of Widely Separated Clocks," Nat. Bur. Standards Tech. Note, Boulder Laboratories No. 22, July 1959
8. Harris, S. M., "Refraction Compensation in a Spherically Stratified Ionosphere," IRE Trans. on Antennas and Propagation AP-9(2):207-210, March 1961
9. Berning, W. W., "Earth Satellite Observations of the Ionosphere," Proc. IRE 47(2):280-288, February 1959
10. Tischer, F. J., "Propagation-Doppler Effects in Space Communications," Proc. IRE 48(4):570-574, April 1960
11. Boudouris, G., "A Method for Interpreting the Doppler Curves of Artificial Satellites," J. British Inst. of Radio Eng. 20(12):933-935, December 1960
12. Habib, E., Kronmiller, G., Engels, P., and Franks, H., "The Goddard Range and Range Rate System," Goddard Space Flight Center Preliminary Report, June 30, 1961

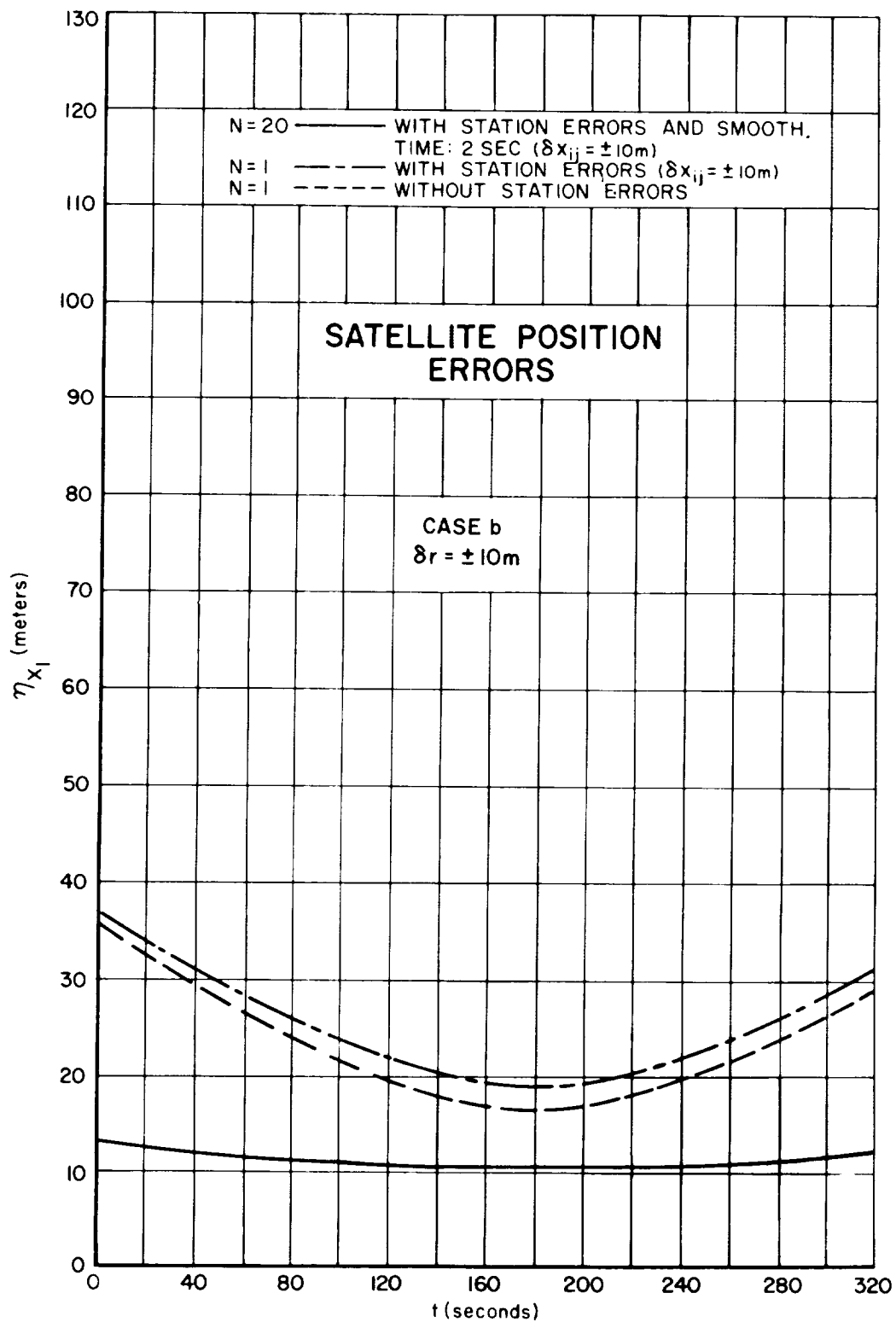


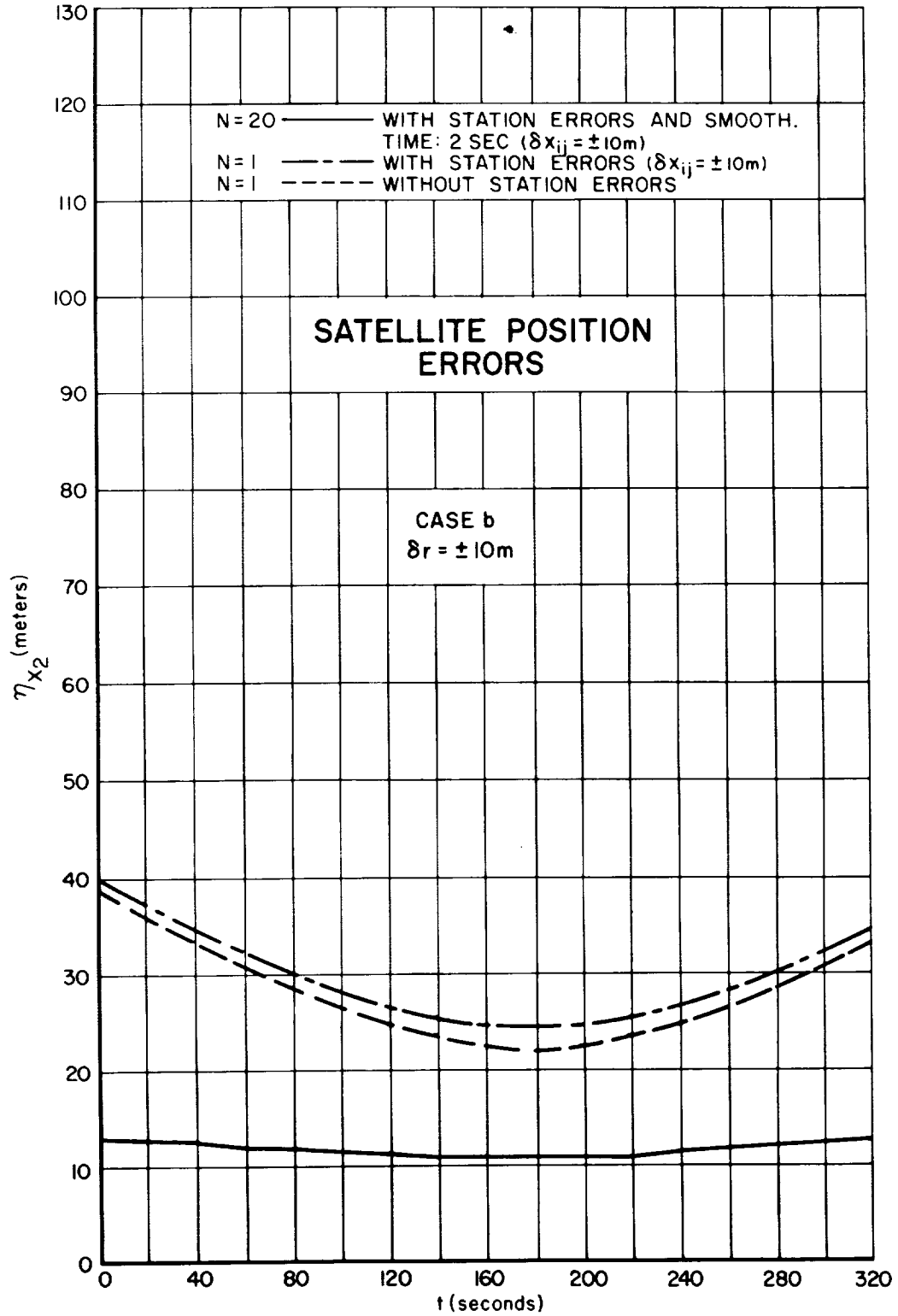


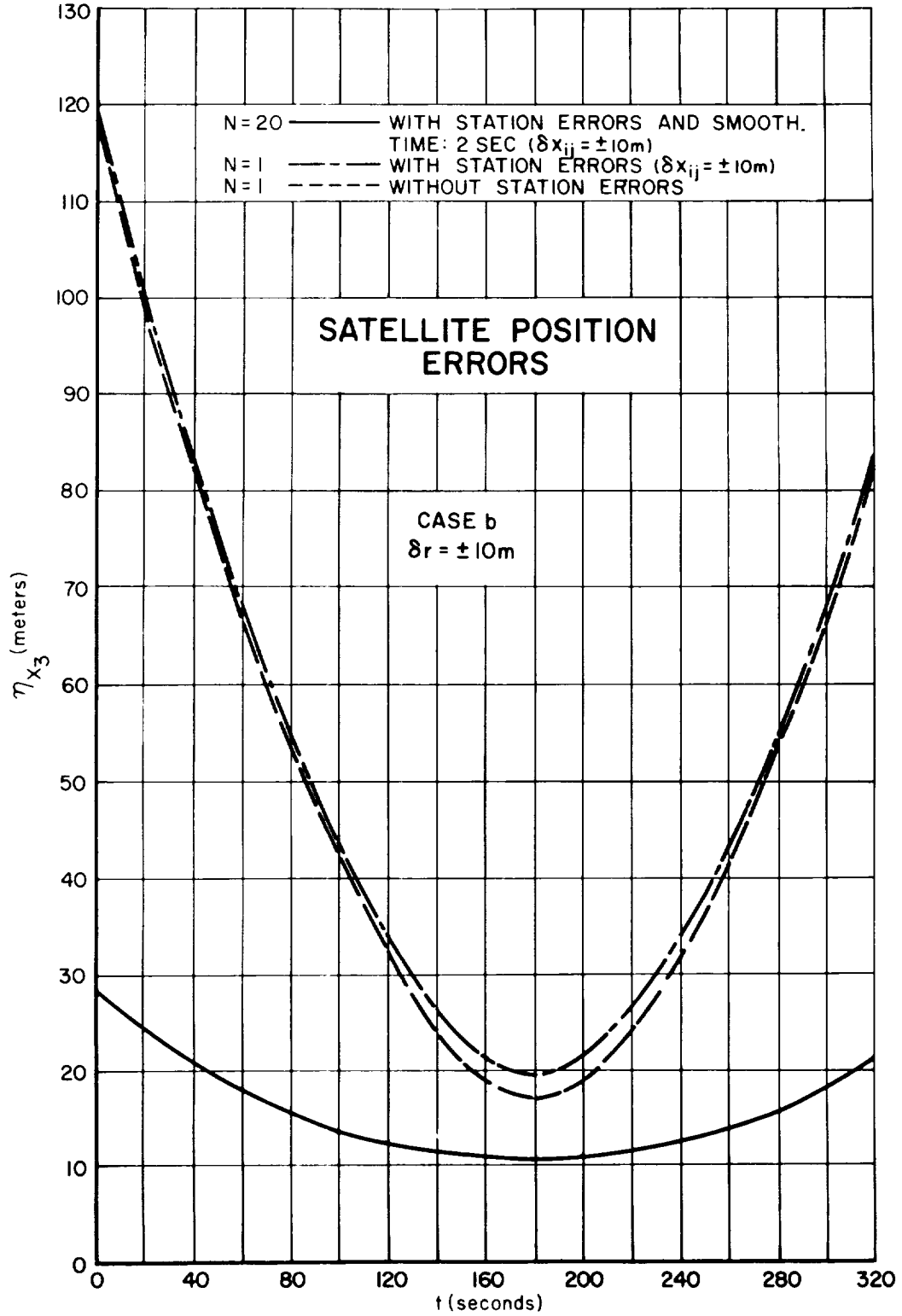


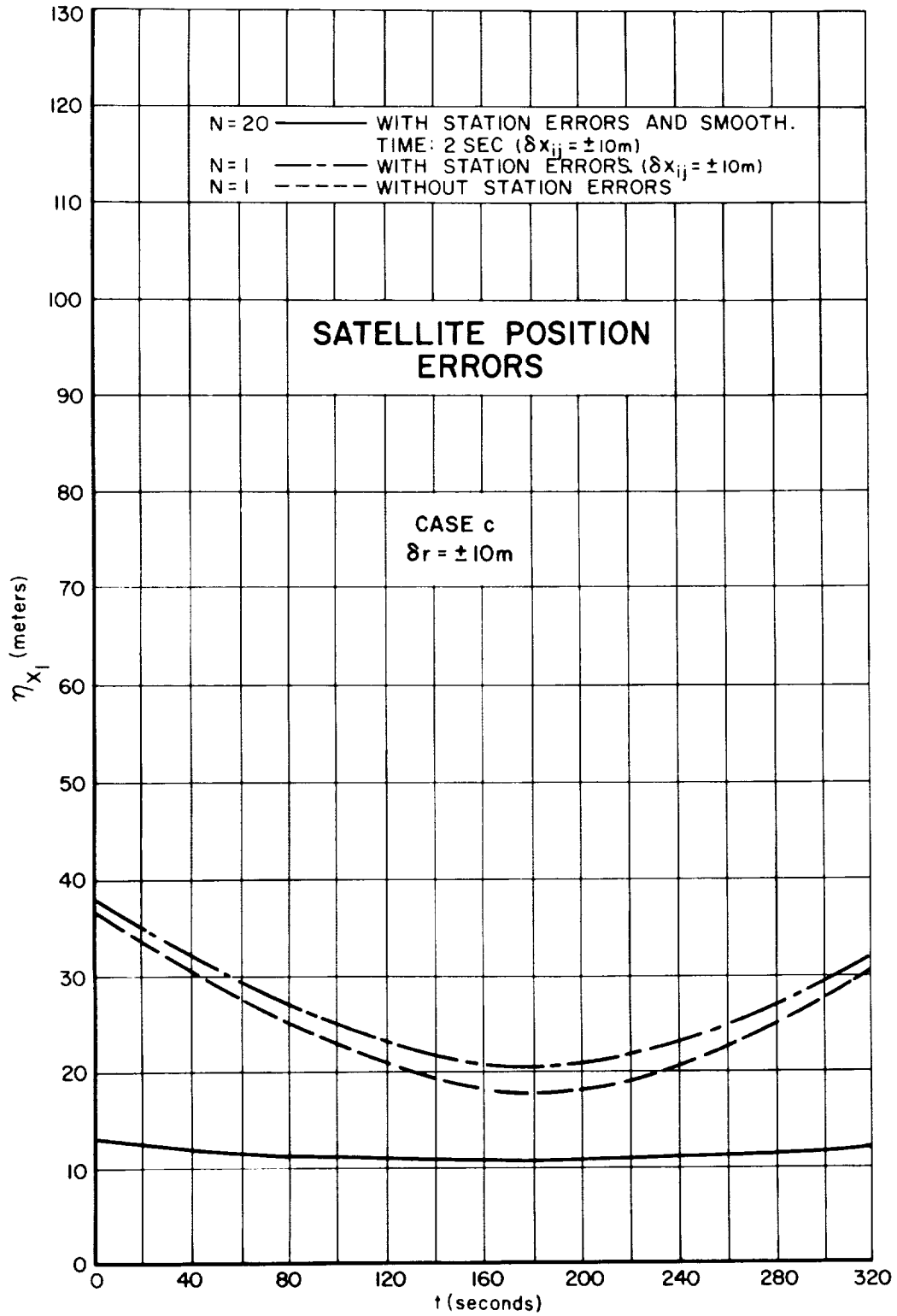


IND-11/8

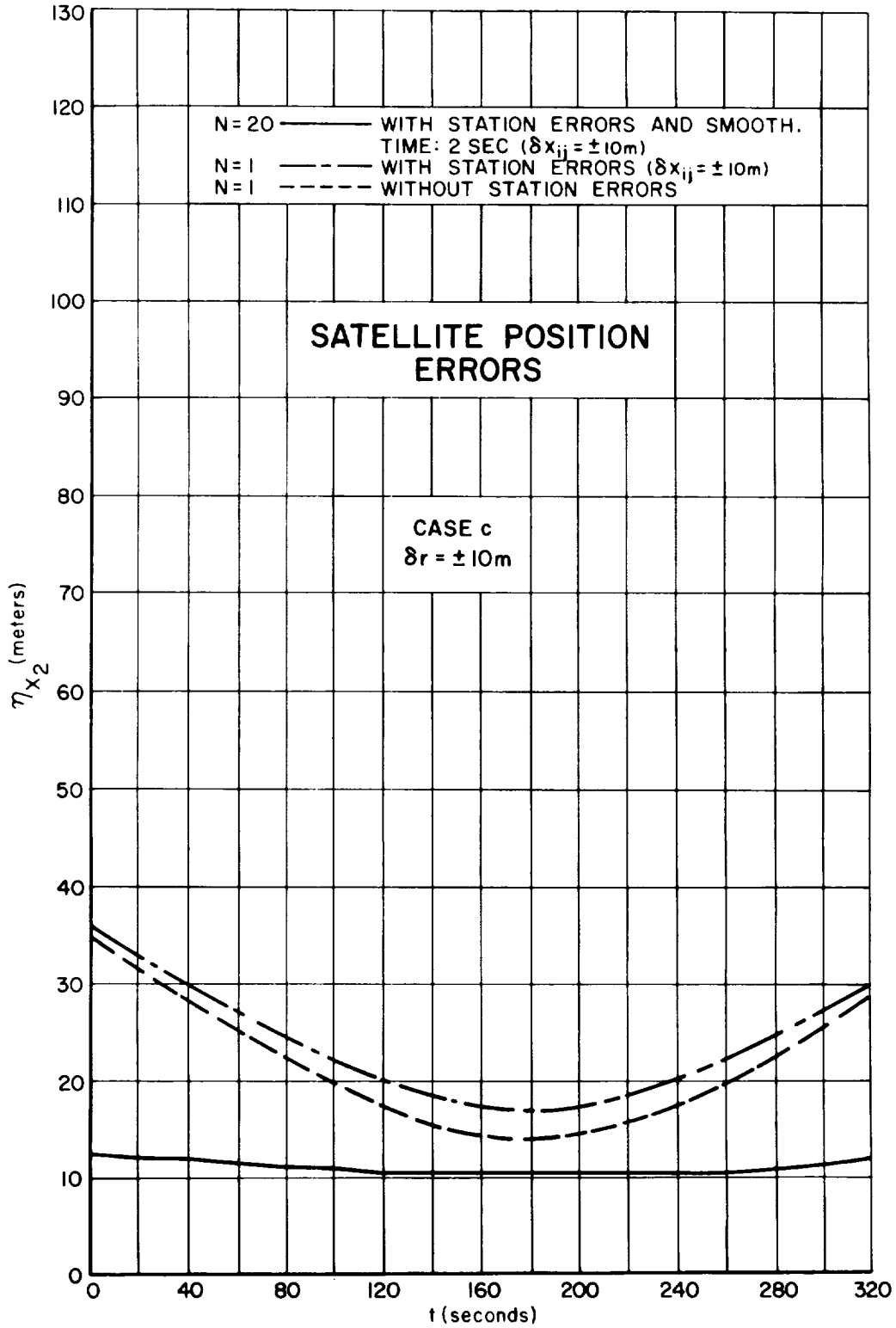


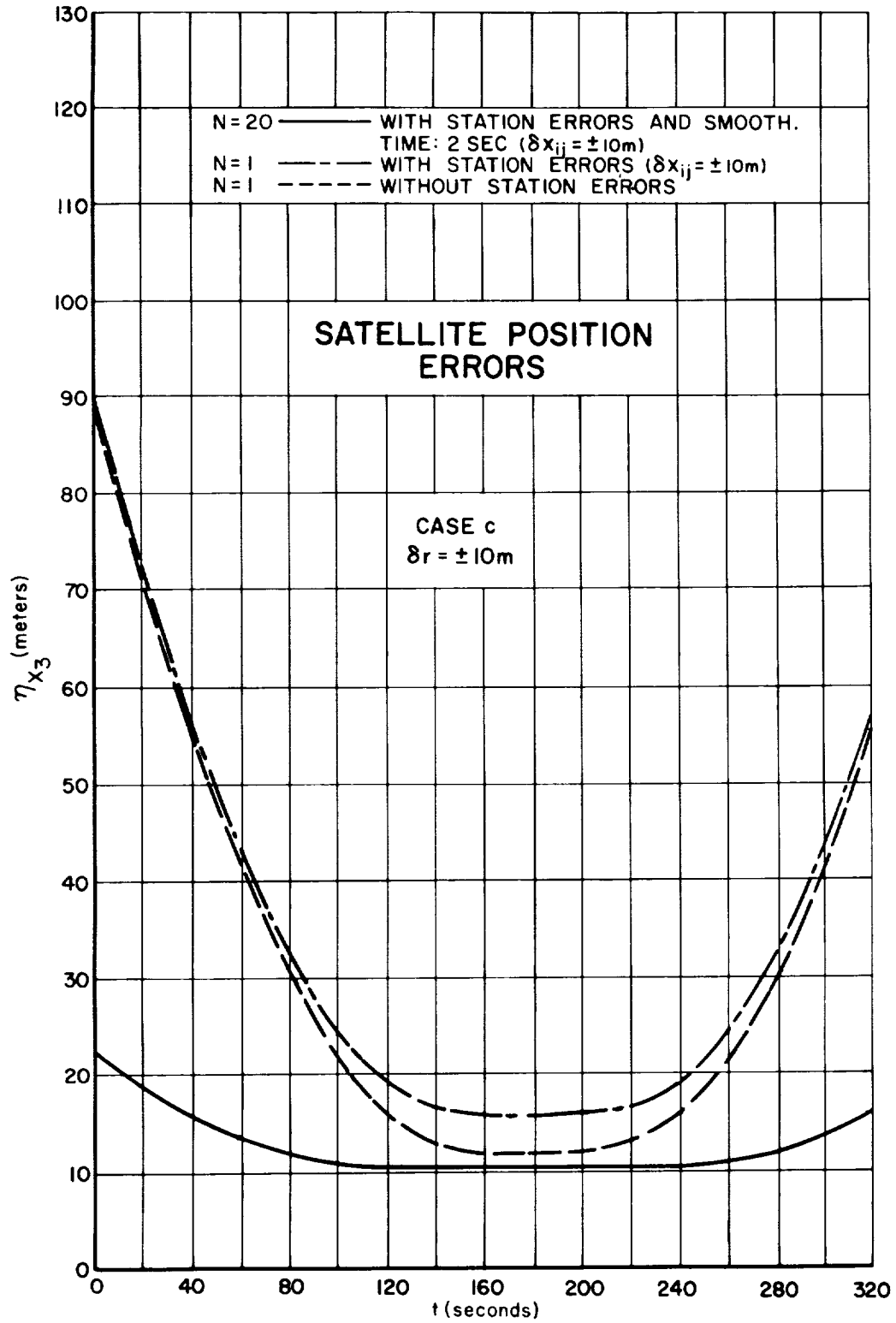


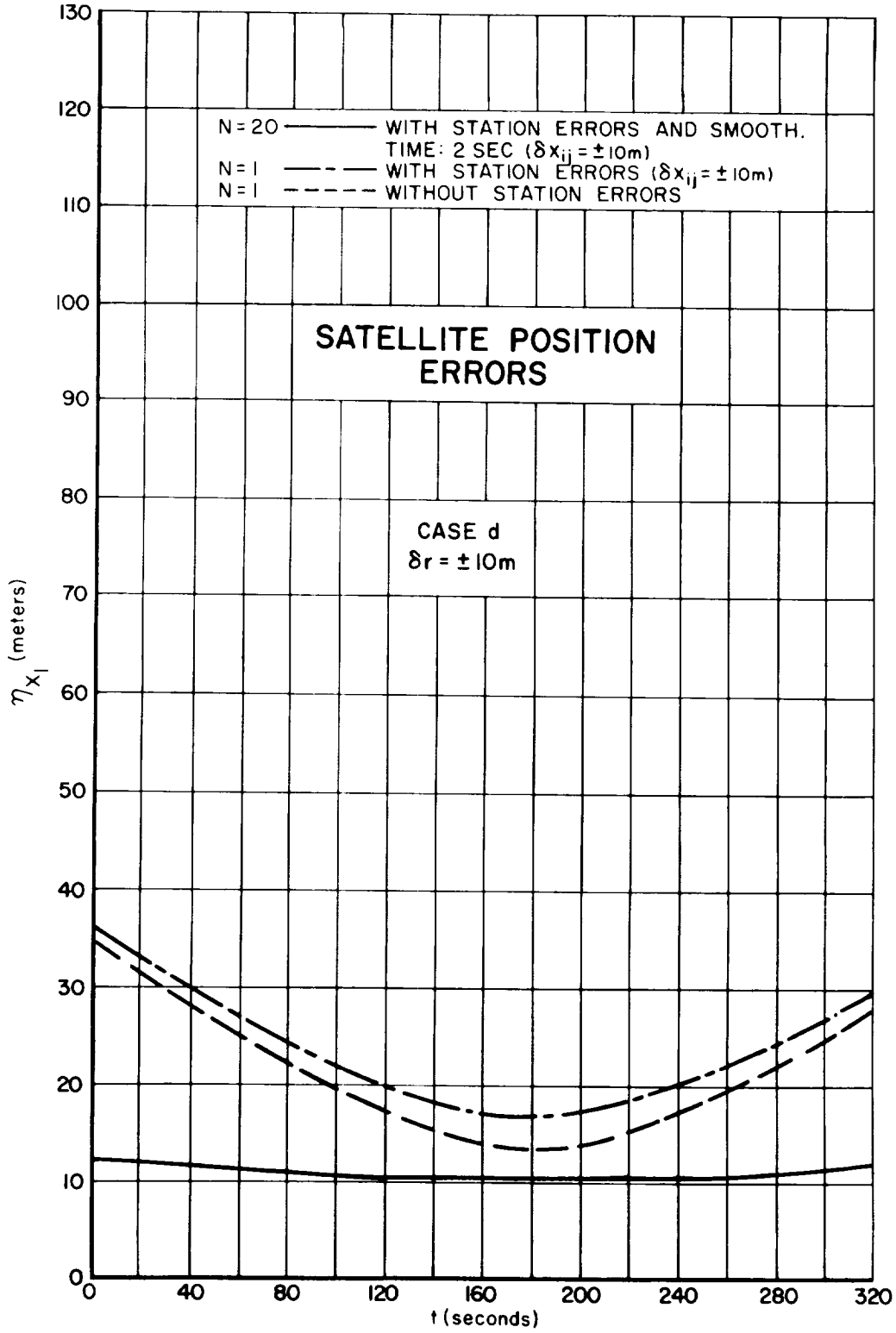


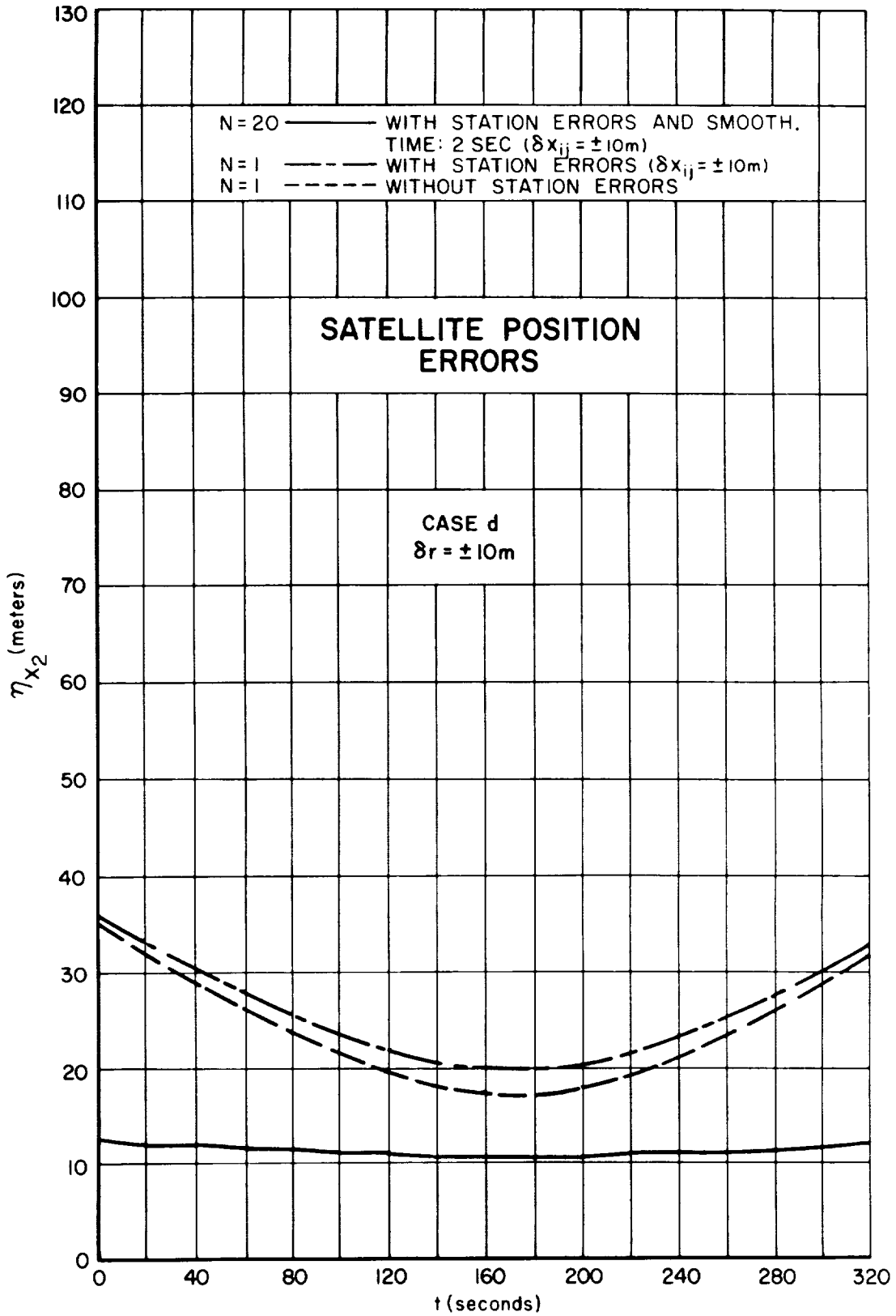


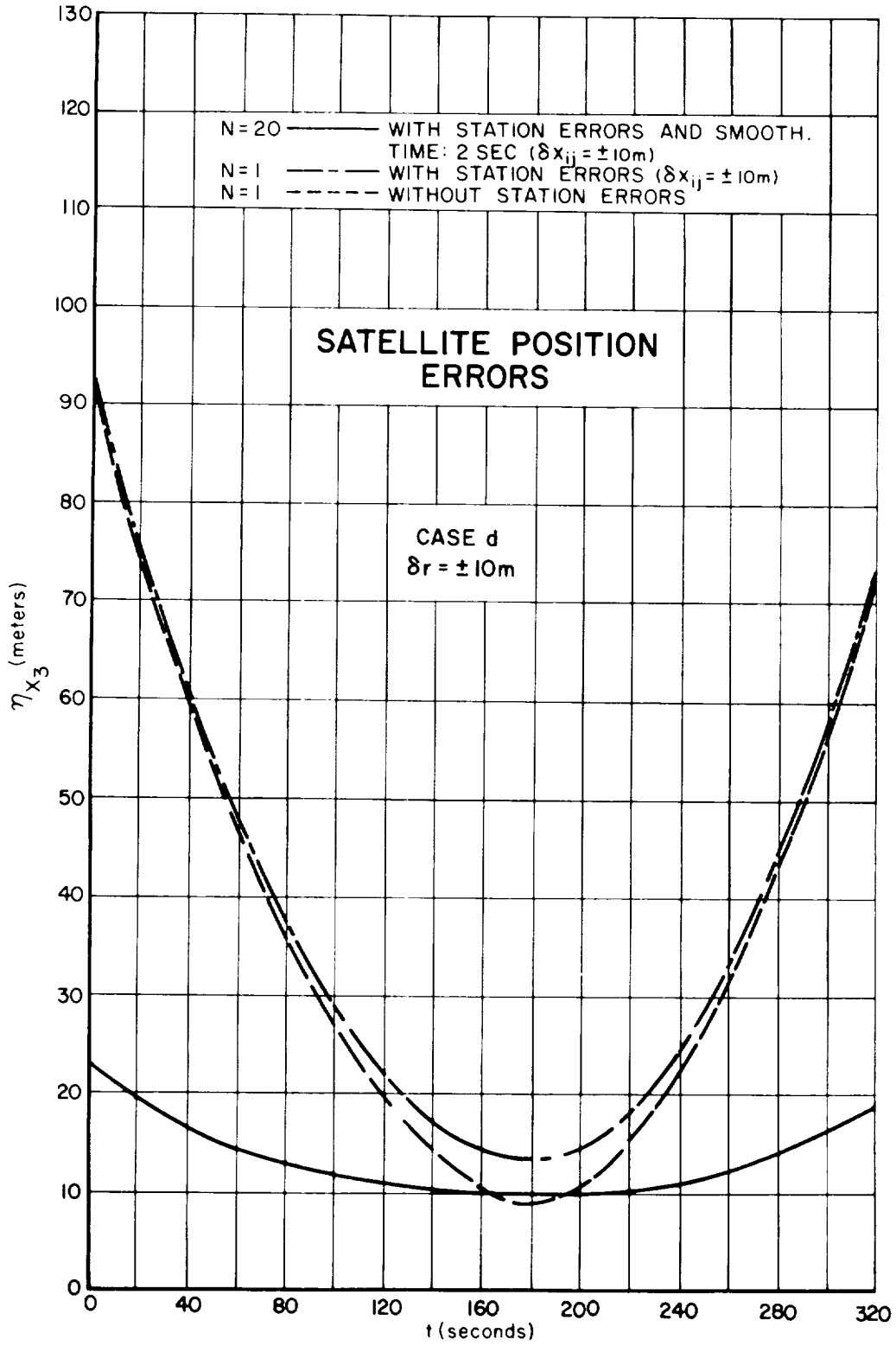
TN D-1178

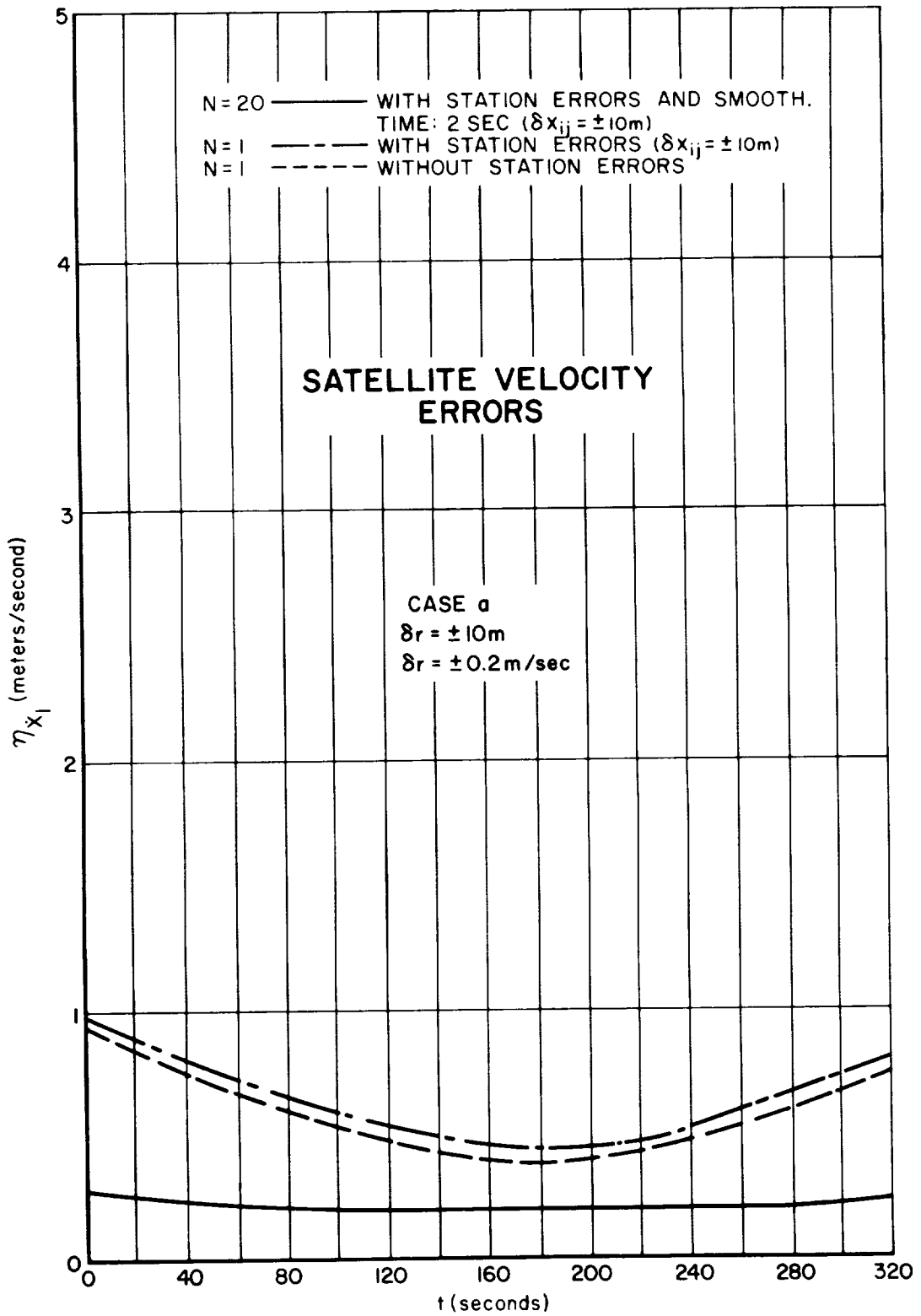








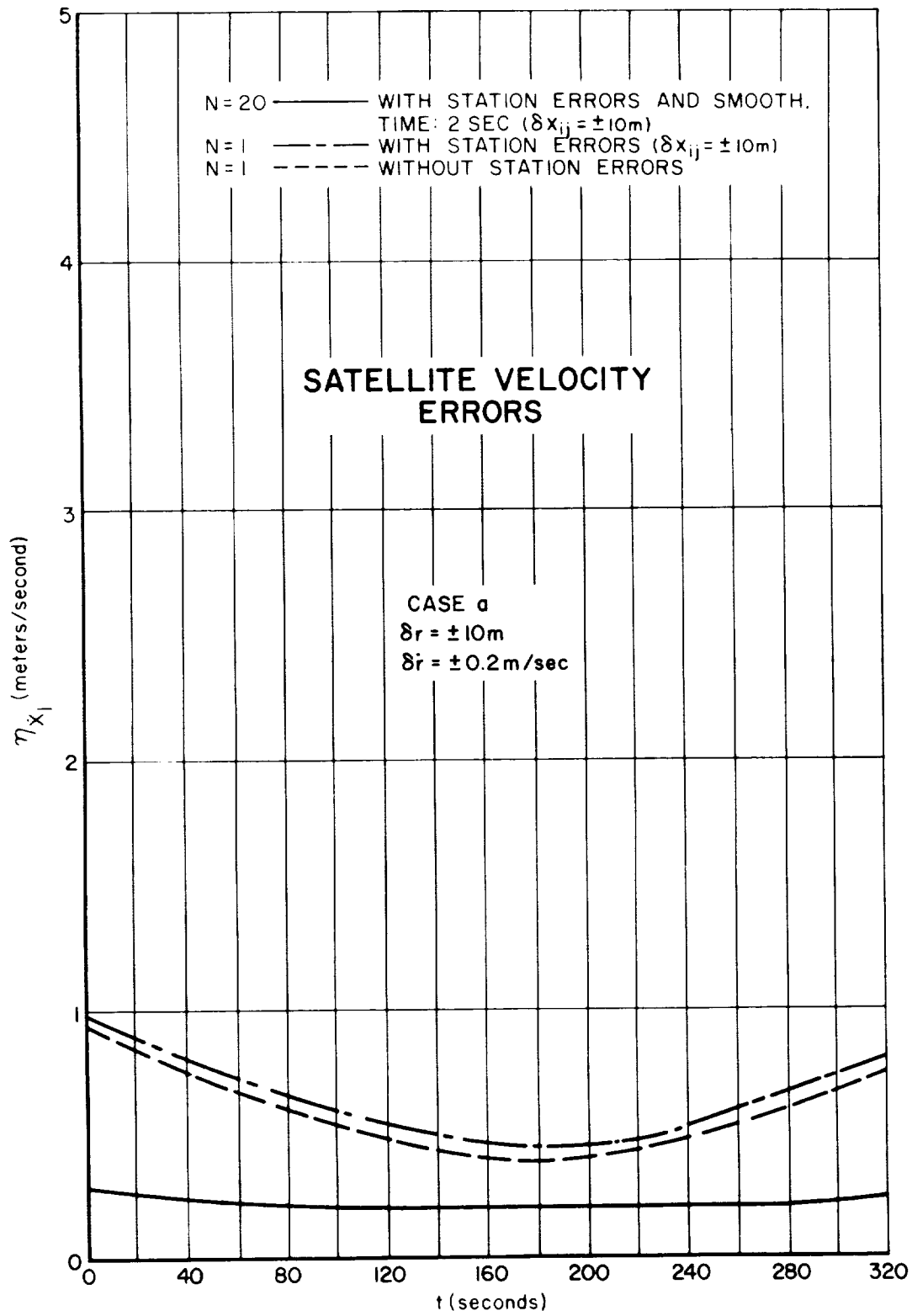




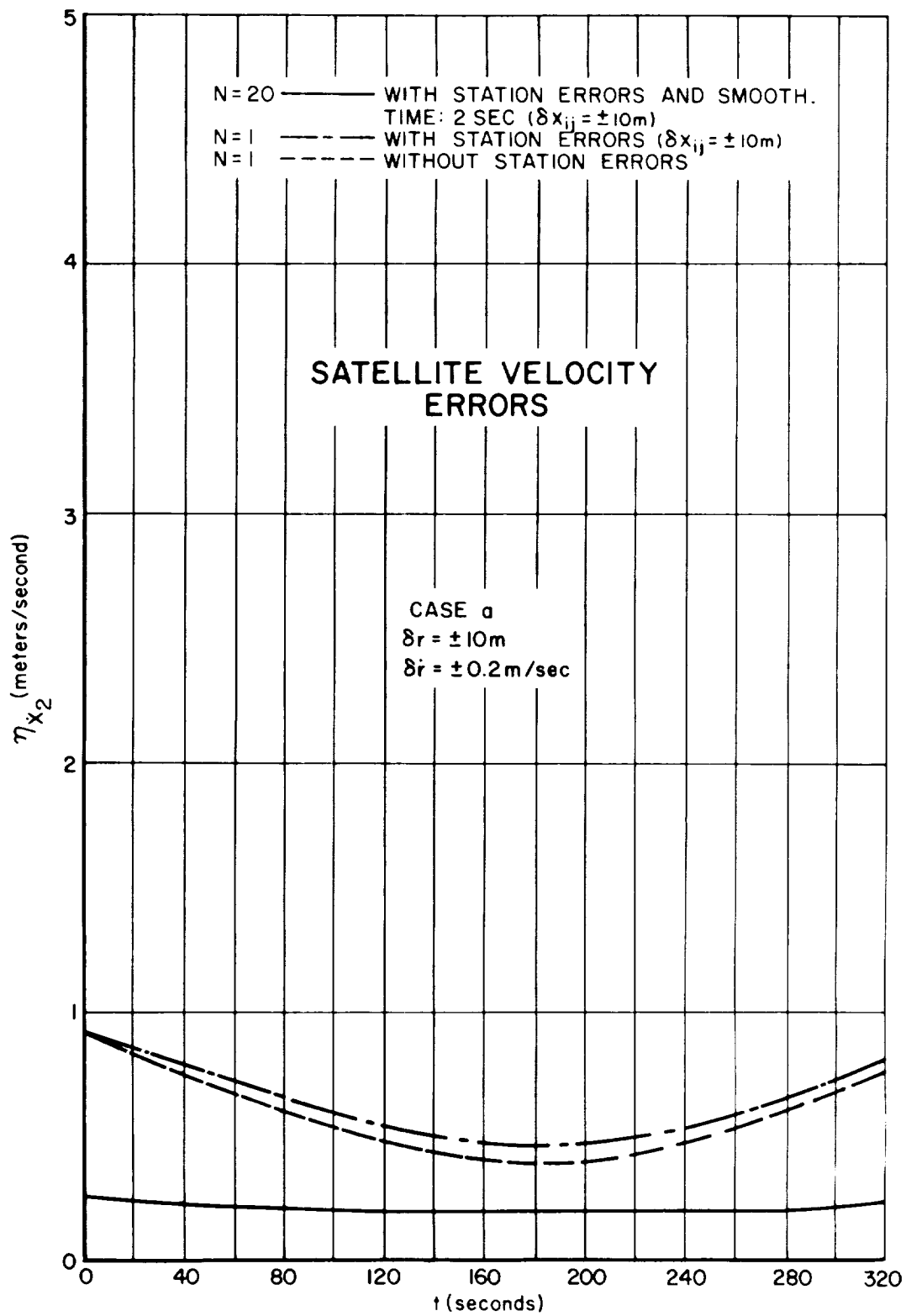
Appendix B

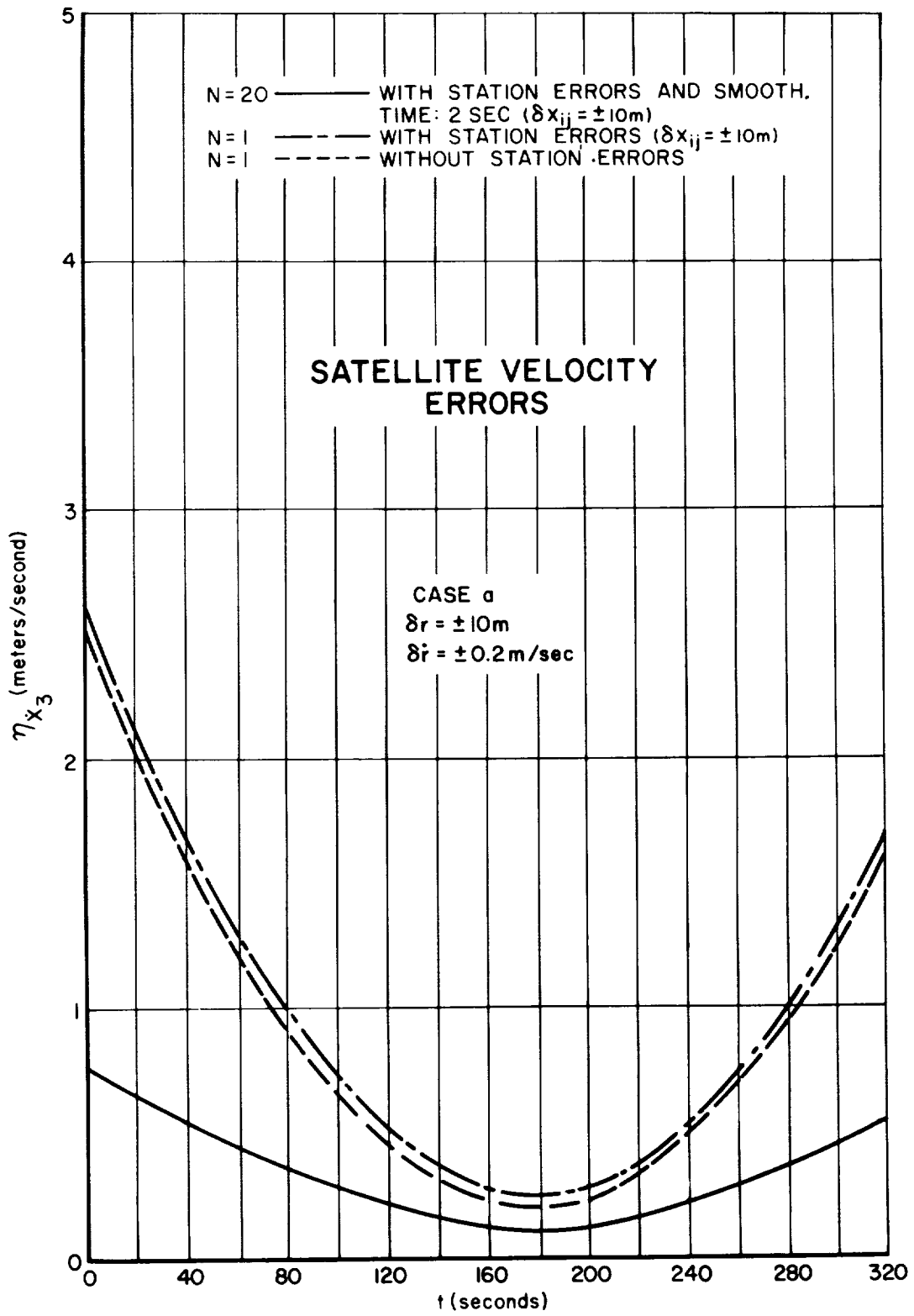
**Details of the Satellite
Velocity Errors**

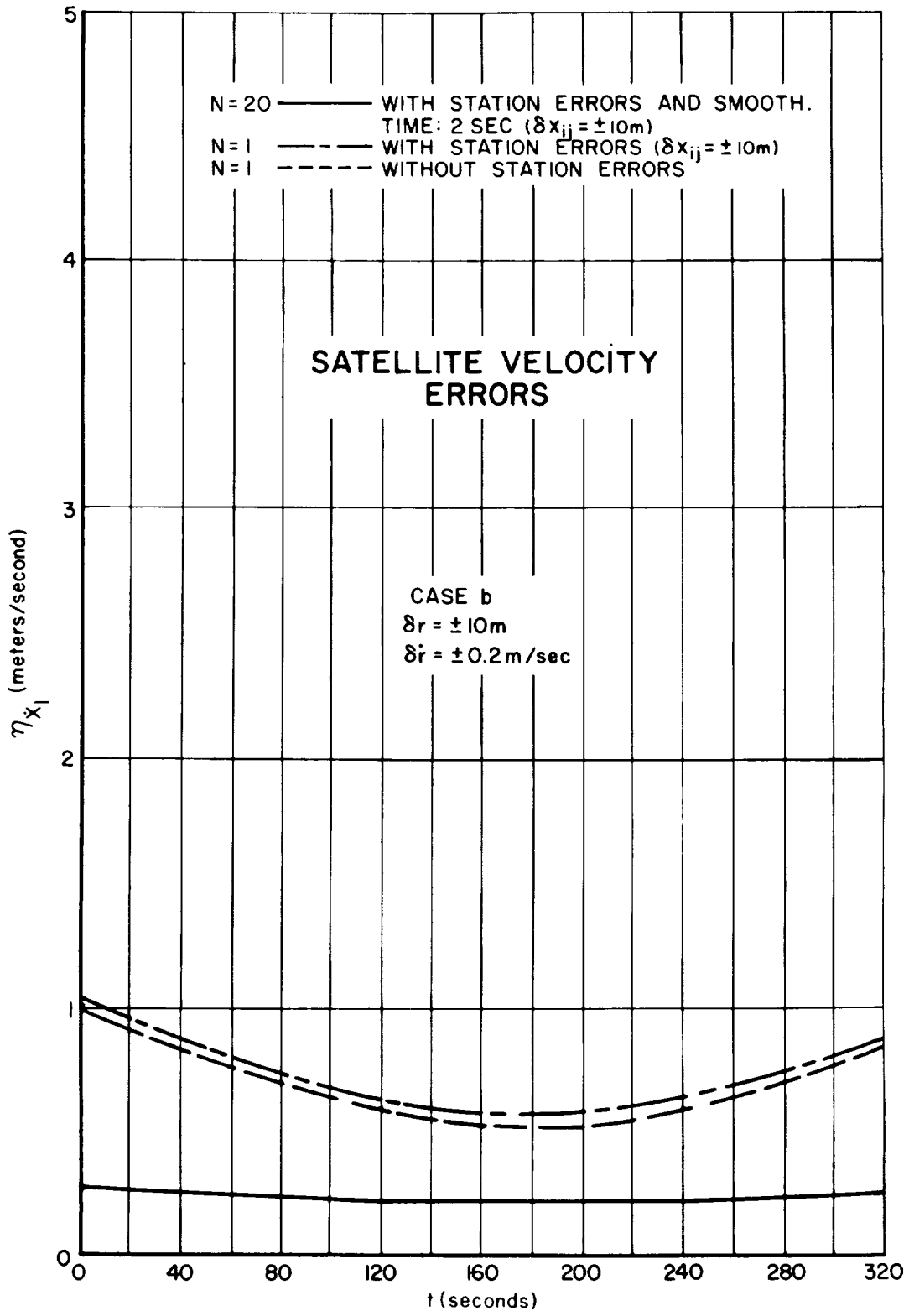
The charts of total satellite velocity errors (Figures 11-14) for Cases a, b, c, and d shown in Figure 5 were constructed from the charts in this appendix.

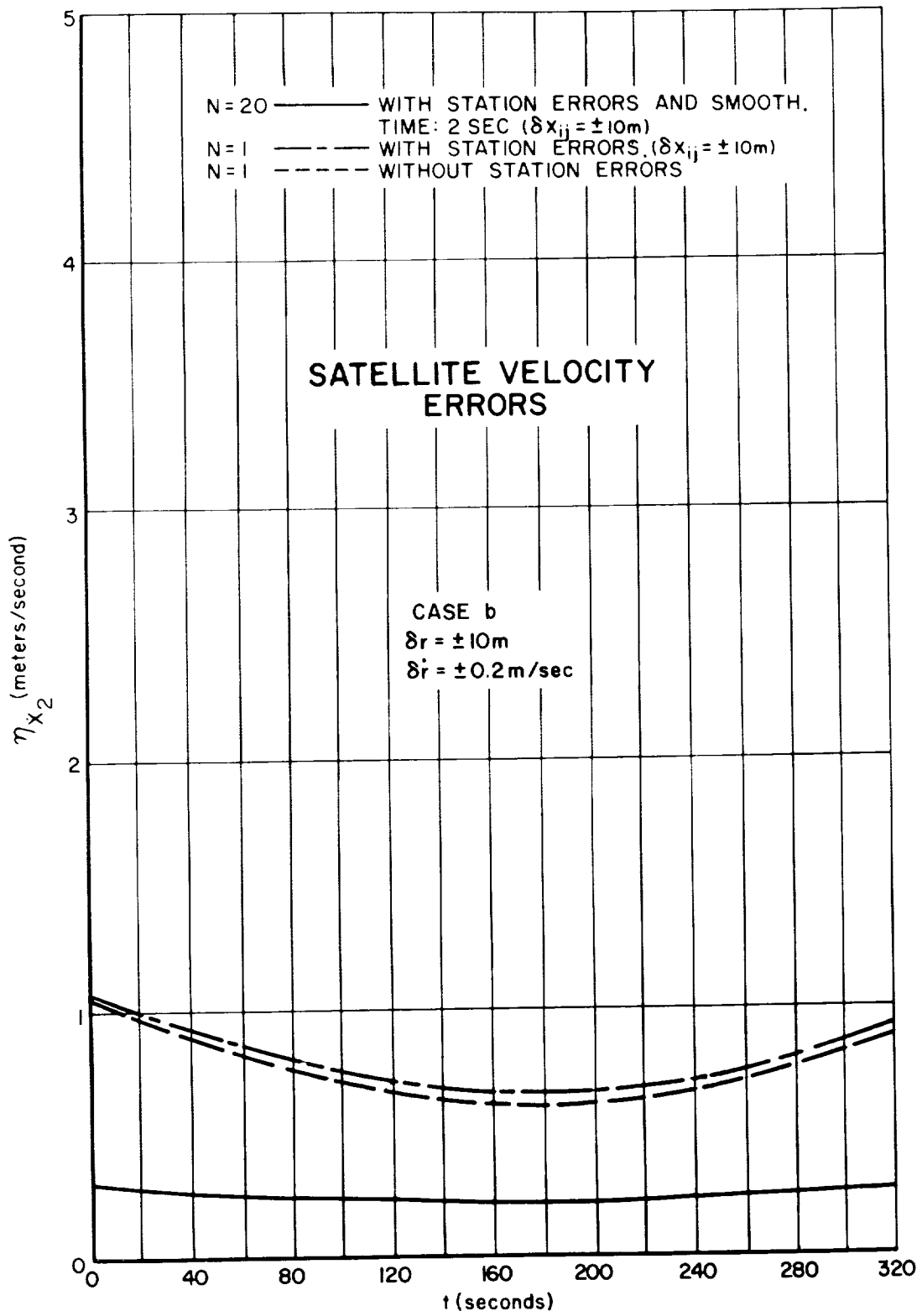


TN D-1178

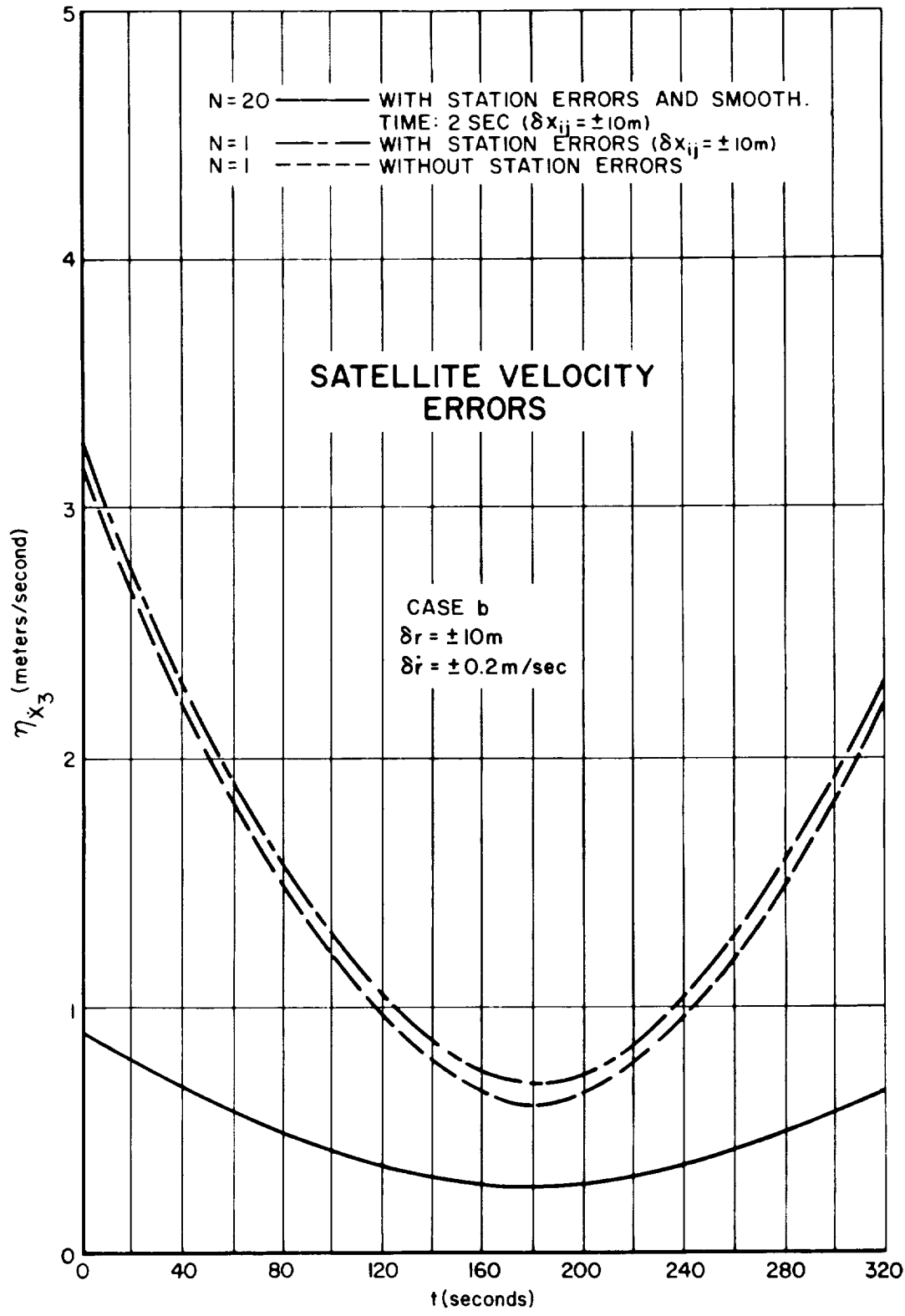


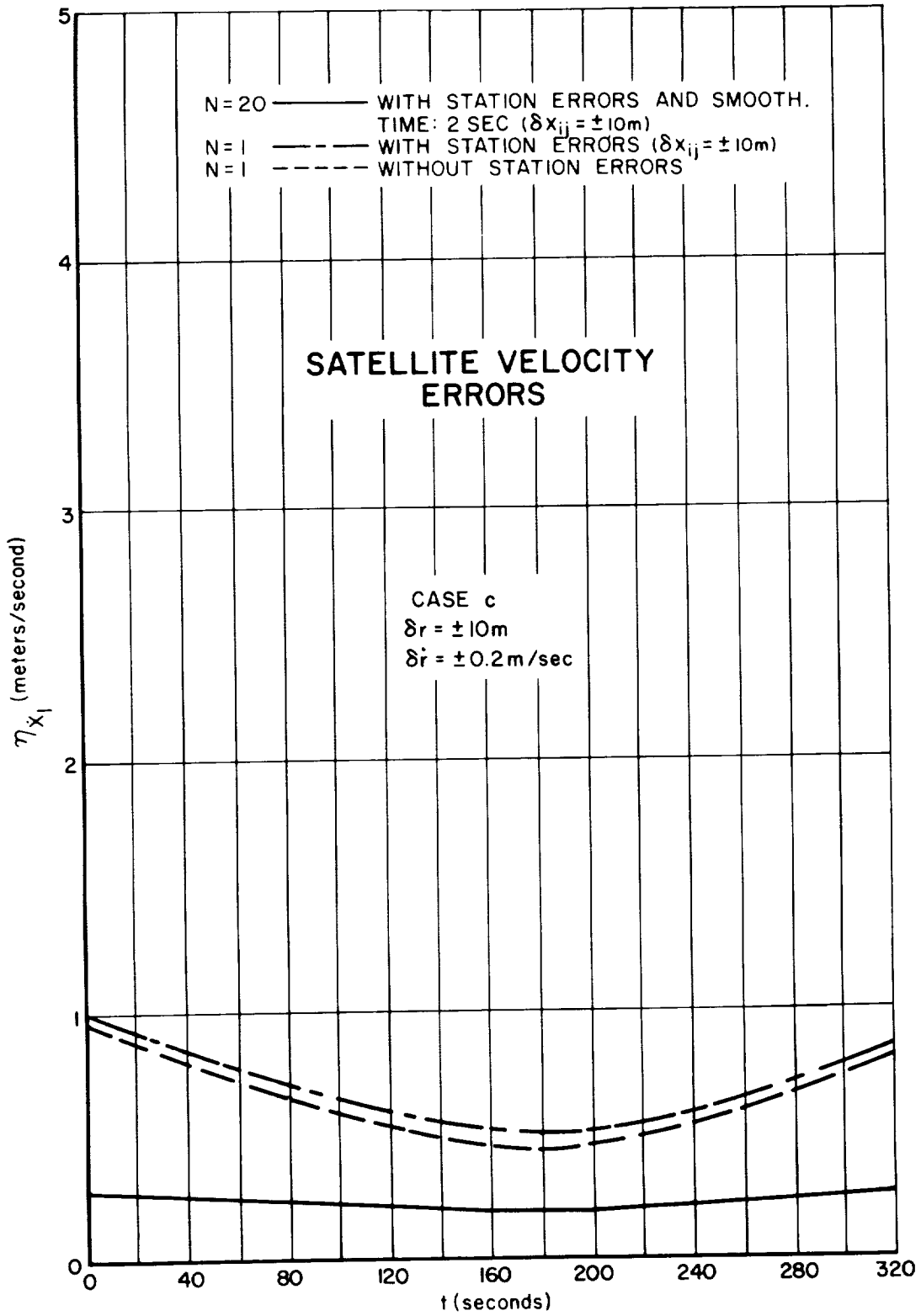




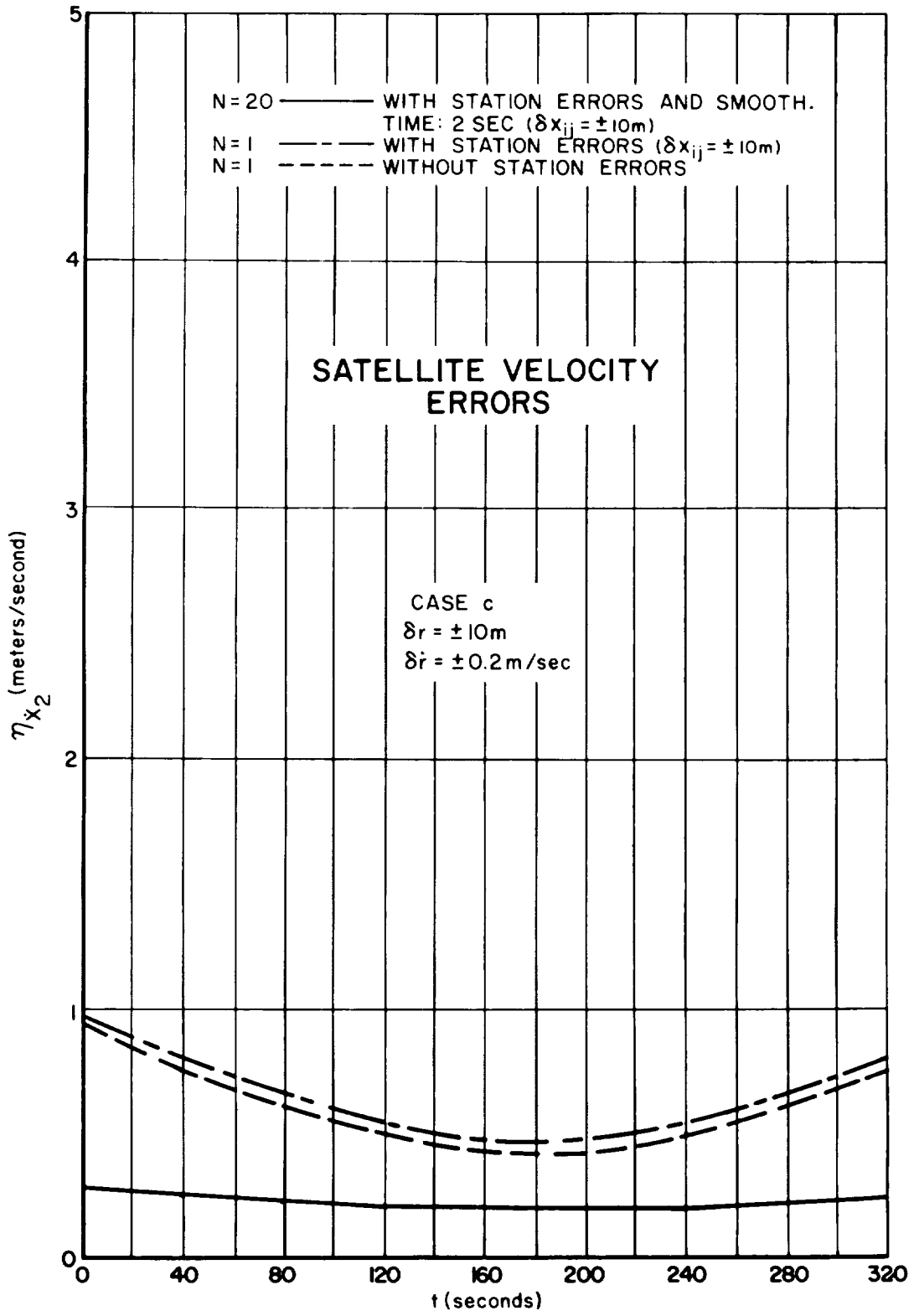


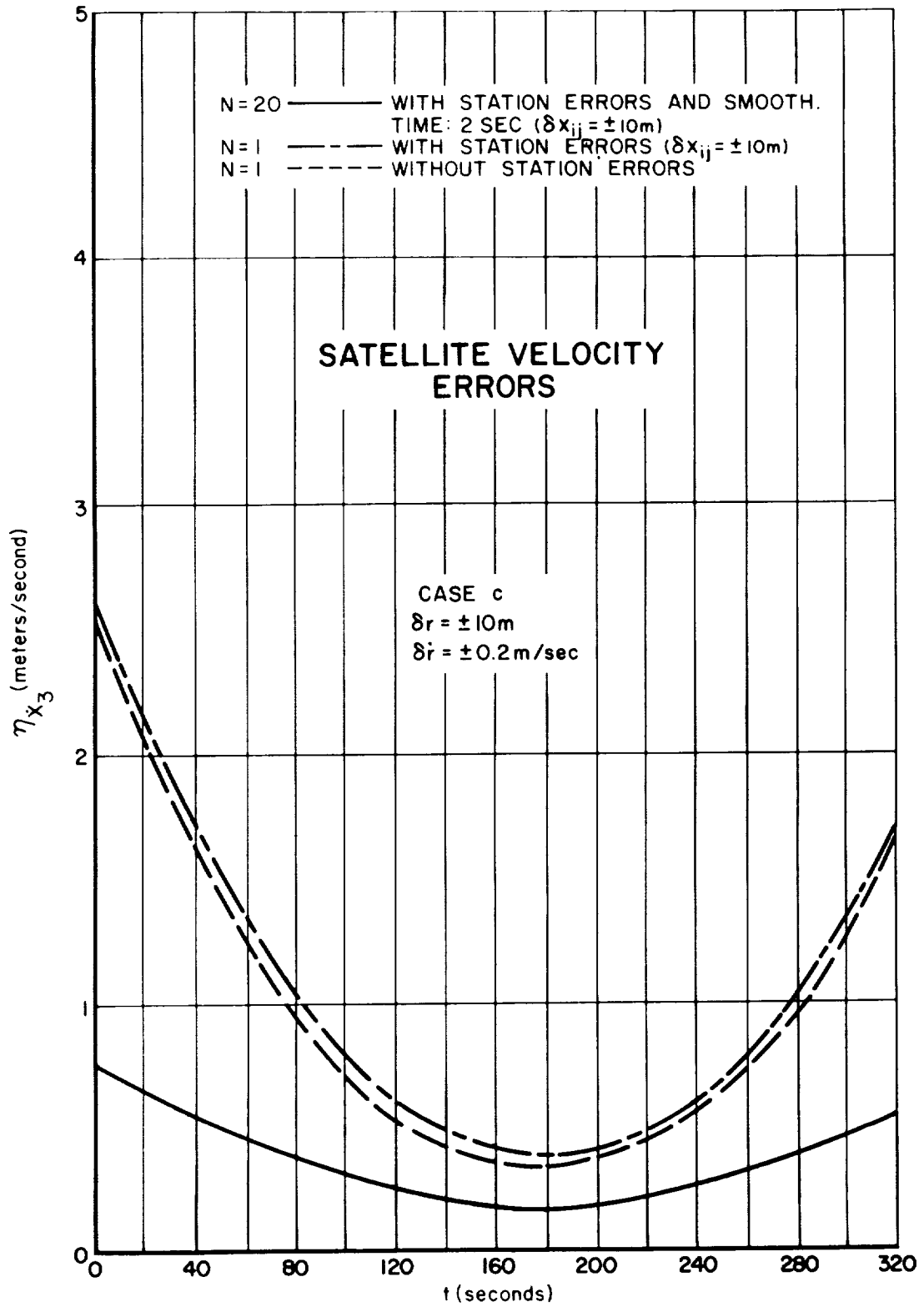
AIN D-1110



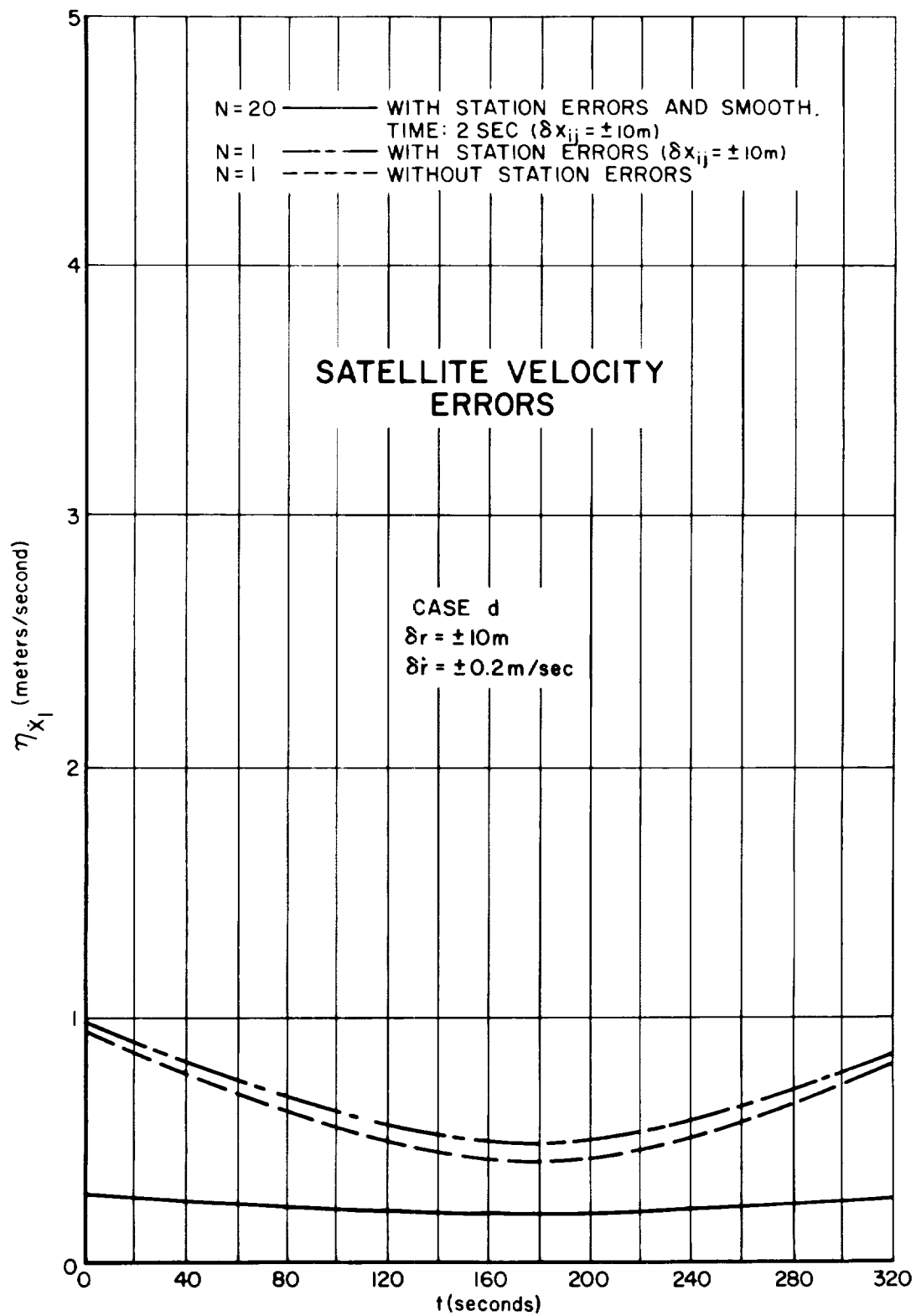


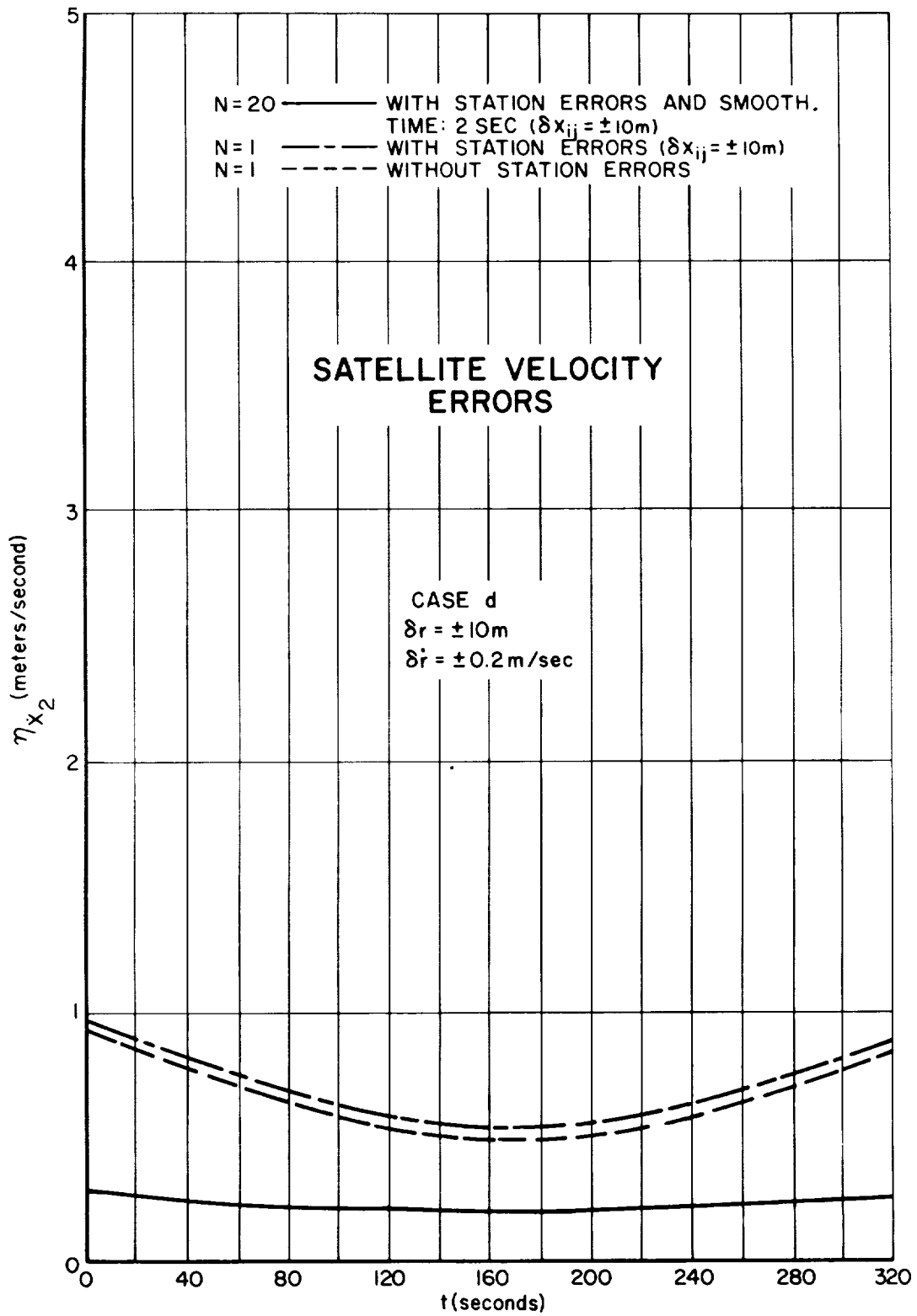
PLAN D-1178





TN D-1178





LIN D-1178

